Available online at www.sciencedirect.com
SCIENCE DIRECT®
Precambrian Research 135 (2004) 251–279
Precambrian Research
www.elsevier.com/locate/precamres

Internal zoning and U–Th–Pb chemistry of Jack Hills detrital zircons: a mineral record of early Archean to Mesoproterozoic (4348–1576 Ma) magmatism

Aaron J. Cavosie[a,*], Simon A. Wilde[b], Dunyi Liu[c], Paul W. Weiblen[d], John W. Valley[a]

[a] *Department of Geology and Geophysics, University of Wisconsin, 1215 W. Dayton St., Madison, WI 53706, USA*
[b] *Department of Applied Geology, Curtin University of Technology, Kent Street, Bentley, WA 6102, Australia*
[c] *Institute of Geology, Chinese Academy of Geological Sciences, 26 Baiwanzhuang Road, Beijing 100037, PR China*
[d] *Department of Geology and Geophysics, University of Minnesota, 310 Pillsbury Drive SE, Minneapolis, MN 55455, USA*

Received 26 February 2004; received in revised form 6 July 2004; accepted 3 September 2004

Abstract

Magmatic processes were important on the nascent Earth during the first 500 million years (Ma) after accretion, yet the causes and timing of this early magmatism are largely unconstrained, as no rocks from this period have been discovered. Rare >4000 Ma detrital zircons from Western Australia preserve the only direct geologic evidence of this early magmatism. To understand the genesis and history of these zircons, we present the results of a combined ion and electron microprobe, and SEM study of the age, Th–U chemistry, cathodoluminescence (CL) zoning patterns, and inclusions for a population of detrital zircons from Jack Hills, Western Australia, with $^{207}Pb/^{206}Pb$ ages ranging from 4348 to 1576 Ma. The majority of the zircons preserve primary growth features discernable by CL imaging, such as oscillatory and sector zoning, have Th/U ratios from 0.1 to 1.0, and several contain granitic mineral inclusions. Thus, aside from age they are largely indistinguishable from zircons produced in common felsic magmas. The Jack Hills zircons are therefore remnants of igneous rock-forming events that pre-date the rock record by up to 400 Ma. The $^{207}Pb/^{206}Pb$ age distribution pattern for zircons older than 3800 Ma from Western Australia suggests that early Archean magmatism was punctuated, both in terms of high frequency events and conspicuous gaps. The variable age distributions within different rock units in the Jack Hills demonstrate that Early Archean zircons were derived from multiple source rocks; samples from Eranondoo Hill contain up to 12% >4000 Ma zircons, suggesting either that the source rocks were nearby or represent a large terrane. Furthermore, younger 3700–3400 Ma rims on 4300–4000 Ma zircons are evidence that >4000 Ma crust survived long enough to participate in younger Archean tectonic events in the Yilgarn Craton of Western Australia. Mesoproterozoic igneous zircons in a quartzite 50 m from Eranondoo Hill are attributed to either sedimentation or

* Corresponding author.
E-mail address: acavosie@geology.wisc.edu (A.J. Cavosie)

0301-9268/$ – see front matter © 2004 Elsevier B.V. All rights reserved.
doi:10.1016/j.precamres.2004.09.001

tectonic interleaving of younger sediments no earlier than 1576 Ma. This previously unrecognized Proterozoic (or younger) geologic history calls into question previous estimates of the age of the Jack Hills sediments and demonstrates the heterogeneous distribution of >4000 Ma grains within the belt.
© 2004 Elsevier B.V. All rights reserved.

Keywords: Jack Hills; SHRIMP; Zircon geochronology; Early Archean; Hadean; Cathodoluminescence; Electric Pulse Disaggregation

1. Introduction

The first 700 million years (Ma) of Earth's history is generally considered to be dominated by a variety of magmatic processes, including planetary accretion, global magma oceans (Tonks and Melosh, 1990), and melting from large impacts (Melosh, 1989). Little evidence of this early global magmatism exists, however, and the ca. 4030 Ma Acasta orthogneisses (Bowring and Williams, 1999) are the oldest known terrestrial rocks. As such, the interval encompassing accretion, core and mantle formation, and the development of crust, hydrosphere, atmosphere, and perhaps the rise of life (Schidlowski, 2001) is nearly absent from the Early Archean rock record. Our usage of the term 'Archean' as the earliest eon of Precambrian time follows IUGS ratified terminology (Plumb, 1991), and Early Archean is here used as a chronometric term to describe the time interval before 3800 Ma, in place of the loosely-defined chronostratic term 'Hadean'. Exposed rocks older than 3800 Ma are uncommon; known occurrences are in Canada and Greenland. However, the discovery of >3800 Ma zircons in Archean sediments worldwide [Froude et al., 1983 (W. Australia); Black et al., 1986 (Antarctica); Liu et al., 1992 (China); Mueller et al., 1992 (USA)] demonstrates that an older Archean record is preserved as detrital minerals, despite the absence of recognized intact rocks. These surviving grains are the oldest known remnants from the early Archean, and can thus provide crucial information about the nature of the earliest formed crust. Estimates of the volume of original >3800 Ma crust have been debated (Nutman, 2001); however, the origins of the >3800 Ma detrital zircons remain unknown. Fundamental aspects of the zircons, such as whether their source rocks were igneous or metamorphic, remain largely unconstrained.

The primary goal of this contribution is to demonstrate that the internal structures and Th–U chemistry provide evidence that >3800 Ma detrital zircons from the Jack Hills, Western Australia, preserve a record of their origins in early Archean magmas — despite long and sometimes complex post-crystallization histories. Demonstrating that the 4350–3800 Ma zircons are igneous in origin allows the identification of rock-forming events in the Early Archean. In addition, Proterozoic detrital zircons identified during this study allow further constraints to be placed on the geologic history of the Jack Hills. The following data are presented: (1) isotopic age determinations for a new suite of detrital zircons from measured sections in the Jack Hills, that range in age from 4348 to 1576 Ma; (2) cathodoluminescence images that allow in situ age determinations to be correlated with internal zoning; (3) $^{207}Pb/^{206}Pb$ age distributions for 4350–3800 Ma zircons from Western Australia, from which early Archean magmatic periods are identified; (4) ages of overgrowths on >4000 Ma zircons that record the participation of Early Archean crust in the evolution of the Yilgarn Craton as late as ca. 3400 Ma; (5) mineral inclusions found within the >4000 Ma zircons identified by energy-dispersive spectroscopy, and (6) zircon age distributions from several locations within the Jack Hills that set new constraints on sediment source and depositional age for the metasedimentary belt.

2. Geologic background

2.1. Jack Hills

The Jack Hills, located in the Narryer Terrane of the Yilgarn Craton in Western Australia (Fig. 1), comprise an ~80 km long northeast-trending belt of folded and metamorphosed supracrustal rocks that are composed primarily of siliciclastic and fine-grained sediments, chemical sediments, and minor mafic/ultramafic rocks (Fig. 2). The siliciclastic portion of the belt has been interpreted as alluvial fan-delta deposits based on repeating fining-upward sequences consisting of

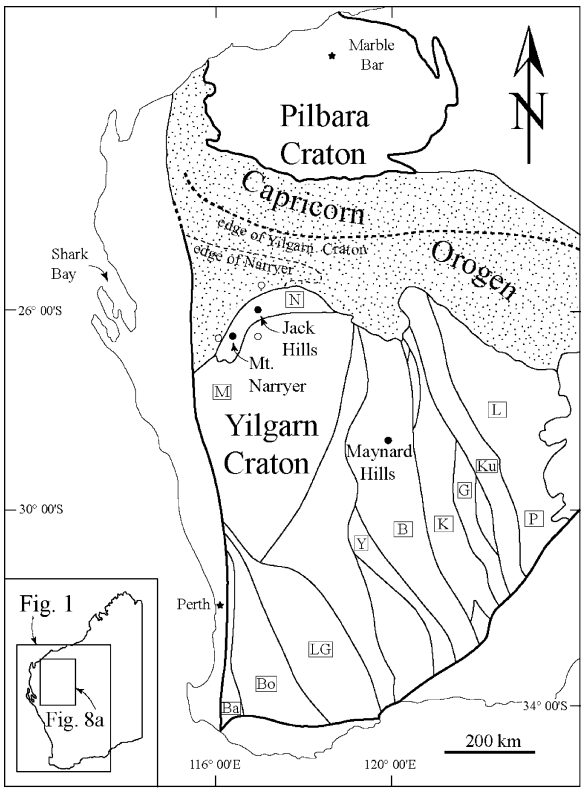

Fig. 1. Map of Archean cratons in Western Australia, after Wilde et al. (1996). Filled circles are known locations of >4000 Ma detrital zircons, open circles are locations of xenocrysts with similar ages (zircon locations referenced in text). Terranes of the Yilgarn Craton — B: Barlee, Ba: Balingup, Bo: Boddington, G: Gindalbie, K: Kalgoorlie, Ku: Kurnalpi, L: Laverton, LG: Lake Grace, M: Murchison, N: Narryer, P: Pinjin, Y: Yellowdine. Dashed lines are inferred boundaries in basement.

basal conglomerate, medium-grained sandstone, and fine-grained sandstones (Wilde and Pidgeon, 1990). Bedding currently strikes east–northeast and has a subvertical dip. The metamorphic history of the Jack Hills is not well known, however the presence of andalusite (Elias, 1983; this study), kyanite (Elias, 1983), and chloritoid (Baxter et al., 1984) suggests the siliclastic rocks experienced greenschist to lower amphibolite facies metamorphism.

The gneisses and granitoids in the Narryer Terrane have been the subject of ongoing geochronology to decipher their complex history, and also to evaluate possible sources for the nearby supracrustal sediments that contain ≥4000 Ma zircons. The oldest identified component of the Narryer Terrane is the Meeberrie gneiss, a complex layered rock (Myers and Williams, 1985) with outcrops from several km north of Jack Hills to 70 km south near Mt. Murchison, yielding a range of igneous zircon ages with discrete populations at 3730, 3680, 3620, and 3600 Ma (Kinny and Nutman, 1996, and references therein; Pidgeon and Wilde, 1998). Included within the Meeberrie gneiss near both Jack Hills and Mt. Narryer are cm–km-scale blocks of a dismembered layered mafic intrusion, called the Manfred Complex (Myers, 1988). Zircons from Manfred Complex samples yielded ages as old as 3730 ± 6 Ma, suggesting it formed contemporaneously with the oldest components of the Meeberrie gneiss (Kinny et al., 1988). Limited exposures of the 3490–3440 Ma Eurada gneiss are found 20 km west of Mt. Narryer, and contain a minor component of younger ca. 3100 Ma zircons (Nutman et al., 1991). South of Jack Hills, the Meeberrie gneiss was intruded by the precursor rocks of the Dugel gneiss, which contain 3380–3350 Ma zircons (Kinny et al., 1988; Nutman et al., 1991), and like the Meeberrie gneiss, contain enclaves of the Manfred Complex (Myers, 1988). Younger granitoids, from 2660 ± 20 to 2646 ± 6 Ma, intrude the older granitoids in the vicinity of Jack Hills and Mt. Narryer (Kinny et al., 1990; Pidgeon, 1992; Pidgeon and Wilde, 1998). Contacts between the Jack Hills metasediments and the older granitoids are sheared, whereas the ca. 2650 Ma granitoids appear to intrude the belt (Pidgeon and Wilde, 1998).

2.2. Review of >4000 Ma detrital zircons

Detrital zircons older than 4000 Ma have only been found in Western Australia.

All three localities are in the Yilgarn Craton (solid dots, Fig. 1): the two areas in the Narryer Terrane are Mt. Narryer (Froude et al., 1983) and Jack Hills (Compston and Pidgeon, 1986), and the third is in the Barlee Terrane, at Maynard Hills (Wyche et al., 2004). In addition, >4000 Ma zircons have been reported as rare xenocrysts in granitoids from three localities in the northwestern Yilgarn Craton and the neighboring Capricorn Orogen (open circles, Fig. 1). Inherited ca. 4000 Ma cores were found in zircons from ca. 3300 Ma gneiss near Jillawarra Bore, north–northeast of Jack Hills (Wiedenbeck et al., 1988), and two >4000 Ma xenocrysts in late Archean granitoids were reported by

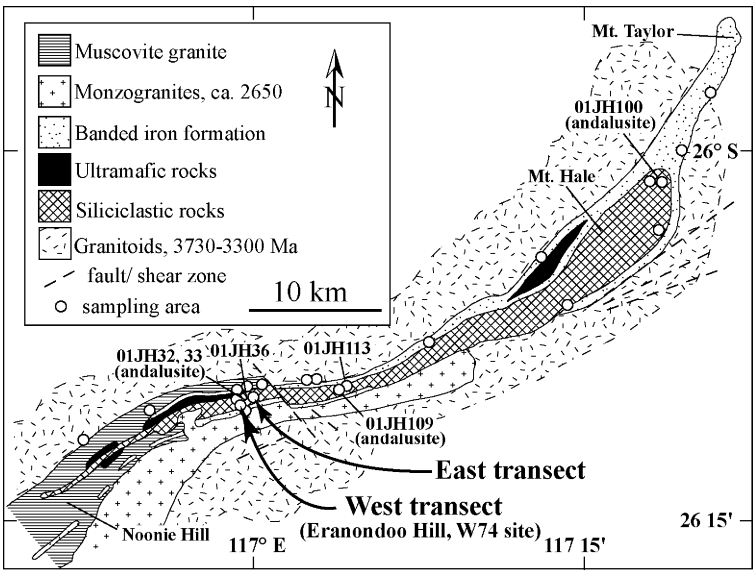

Fig. 2. Simplified geologic map of the Jack Hills metasedimentary belt, after Wilde and Pidgeon (1990).

Nelson et al. (2000); one from a 2636 ± 4 Ma granitoid 20 km west of Mt. Narryer, and another from a 2689 ± 16 Ma granitoid 40 km south of Jack Hills in the Murchison Terrane. Of the above-mentioned localities, only Mt. Narryer and Jack Hills have yielded multiple grains over 4000 Ma from multiple samples (Froude et al., 1983; Compston and Pidgeon, 1986; Kober et al., 1989; Maas et al., 1992; Nelson, 2000; Wilde et al., 2001; Mojzsis et al., 2001; Peck et al., 2001). At Jack Hills, these zircons comprise up to 12% of a given population studied, whereas at Mt. Narryer they have not exceeded 4% of studied grains (see above references). In all cases, no original host rock for these zircons has been recovered, leaving the nature of their source rocks open to speculation.

Early studies shared the common interpretation that the >4000 Ma zircons originated in igneous rocks. This conclusion was based primarily on grain morphologies and Th and U abundances and/or ratios. However, inferred magma compositions have been controversial. Froude et al. (1983) identified four >4000 Ma zircons from Mt. Narryer and provided a transmitted light picture of one angular 4110 Ma detrital zircon fragment, and concluded they originated in silica-saturated rocks. In a subsequent study of seventeen 4276–3920 Ma detrital zircons from Jack Hills, Compston and Pidgeon (1986) noted the rounded forms, lack of internal zoning and inclusions, and low average U (100 ppm) and Th (50 ppm) contents and proposed a mafic source. The first published images of Jack Hills zircons are reflected light pictures of 18 grains, with four older than 4000 Ma (Kober et al., 1989). The four >4000 Ma zircons were consumed during analysis by the thermal ionization Pb-evaporation method, and are interpreted as originating in a tonalite/granodioritic source based on $^{208}Pb/^{206}Pb$ ratios (Kober et al., 1989). Kinny et al. (1990, p. 54) reported that four of the >4000 Ma grains reported by Froude et al. (1983) from Mt. Narryer were later found to have younger ca. 3900 Ma rims, which they interpreted as metamorphic, although neither the rims nor the U/Pb ages have ever been documented. A study by Maas et al. (1992) on sixteen 4192–3908 Ma detrital zircons from Jack Hills and Mt. Narryer describes their simple internal structures, faint euhedral zoning, 'granitic' polyphase inclusions (including quartz, K-feldspar, biotite, chlorite, amphibole, apatite, and monazite), 'crustal' Sc concentrations (up to 46 ppm in cores; analyses by electron microprobe), and high U (up to 650 ppm), and concludes the zircons originated in felsic continental rocks.

While several of the above studies mentioned optical zoning in the >4000 Ma zircons, the extent of internal structure was not realized until the application

of electron beam techniques, such as cathodoluminescence (CL) and back-scattered electron (BSE) imaging, and further established by correlating these images with targeted in situ analyses. The first CL images of Early Archean zircons from the Yilgarn Craton, which included the locations of both U/Pb and trace element analyses, were published by Nelson et al. (2000) for the two >4000 Ma xenocrysts found in younger granitoids from near Mt. Narryer. Igneous oscillatory zoning is preserved in the cores of the crystals, and correlates with zoning of minor and trace elements. Wilde et al. (2001) and Peck et al. (2001) published the first CL images of a >4300 Ma detrital zircon, a grain from Jack Hills with one spot as old as 4404 Ma, and identified on it the locations of the U/Pb, REE, and oxygen isotope analyses, as well as the locations of quartz inclusions. The authors interpreted oscillatory zoning surrounding an original inner core in the CL image as correlating with zoning in both δ^{18}O and REE, features consistent with igneous processes in a quartz-saturated magma (Peck et al., 2001).

Thus far, three crystals have extended the mineralogical record beyond the 4276 ± 6 Ma grain originally reported by Compston and Pidgeon (1986) from Jack Hills: a 4404 ± 4 Ma grain from Jack Hills (Wilde et al., 2001), a 4364 ± 4 Ma grain from the Barlee Terrane (Wyche et al., 2004), and a 4284 ± 6 Ma grain, also from Jack Hills (Mojzsis et al., 2001). Where these zircons originated, what kind of rocks they were eroded from, and how they were transported and incorporated into their sedimentary hosts remains unknown.

2.3. Characterizing detrital zircons

Zircon is a ubiquitous accessory mineral that forms in a wide range of geologic environments and rock types. Identifying the origins of detrital zircons requires the recognition of characteristics that are useful for discriminating between different petrogenetic environments. While the most common primary occurrence of zircon is in felsic to intermediate composition igneous rocks, zircon can precipitate, dissolve, or recrystallize during metamorphic and/or hydrothermal processes (Hoskin and Schaltegger, 2003), and can survive many cycles of melting and sedimentation.

Several features have been described that appear diagnostic of igneous zircon, including growth zoning patterns, Th/U ratios, REE, and δ^{18}O (for recent reviews, see Cox, 2002; Corfu et al., 2003; Hoskin and Schaltegger, 2003; Valley, 2003). Much attention has focused on the use of REE patterns in zircons for discriminating between igneous source rocks (Hoskin and Ireland, 2000; Belousova et al., 2002) and the use of δ^{18}O for detecting different source contributions and/or subsolidus alteration of igneous rocks (Valley et al., 1994, 2002; Valley, 2003). However, in this report we emphasize that internal zoning patterns and Th–U chemistry can be used to distinguish igneous from non-igneous zircon. With this in mind, the main goal of this paper is to constrain broadly the origins of the Jack Hills detrital zircons.

Several types of growth zoning patterns have been described in igneous zircons that are readily discernable in CL images. The most common growth zoning patterns are oscillatory (concentric, euhedral) and sector (hourglass, fir-tree) zoning (Pidgeon, 1992; Hanchar and Miller, 1993; Vavra et al., 1999; Hoskin, 2000; Corfu et al., 2003). No non-magmatic mechanism has been demonstrated to produce oscillatory zoning in zircon (Hoskin, 2000). Non-magmatic zircon (i.e. metamorphic, recrystallized, or hydrothermal) tends to have poorly-defined internal zoning, and may show non-geometric patchy zoning (Pidgeon, 1992; Hanchar and Miller, 1993; Hoskin and Black, 2000). Igneous zircon also tends to form euhedral crystals or euhedral overgrowths on preexisting grains. In contrast, metamorphic zircon morphology is highly variable, and typically has rounded cores and/or rims (Pidgeon, 1992; Hanchar and Miller, 1993), but can form euhedral crystals (Chiarenzelli and McLelland, 1993), and new growth of zircon is sometimes difficult to distinguish from recrystallized zircon (Hoskin and Black, 2000).

Igneous zircon has characteristically higher Th/U ratios that usually do not overlap with Th/U ratios of non-igneous zircons. Williams and Claesson (1987) first demonstrated the utility of the Th/U ratio for distinguishing primary igneous zircons by showing that the Th/U ratios of zircons from paragneisses varied systematically from the so-called igneous crustal values of 0.1–1.5 in cores, to much lower 'metamorphic' values of 0.01–0.1 in the overgrowths. The characteristic of igneous zircons having Th/U ratios >0.1 has been noted in several subsequent studies (Vavra et al., 1996; Hoskin and Black, 2000; Hartmann and Santos, 2004).

3. Sample descriptions

Previous studies from Jack Hills found >4000 Ma zircons from the same aliquot of the original W74 composite sample collected on Eranondoo Hill by Wilde, Pidgeon and Baxter in 1984 (Compston and Pidgeon, 1986; Kober et al., 1989; Amelin, 1998; Amelin et al., 1999; Wilde et al., 2001; Peck et al., 2001; Valley et al., 2002), or additional samples from the same 2 m thick outcrop (Maas and McCulloch, 1991; Maas et al., 1992; Nelson, 2000; Mojzsis et al., 2001). New samples were collected for this study, with one of the goals being to determine the distribution of >4000 Ma zircons in different lithologic units away from the original W74 site. Over 100 samples were collected from the Jack Hills, including 22 from transects of two selected stratigraphic sequences, located 900 m apart in the siliciclastic section in the southwest part of the belt (Fig. 2). These two transects were chosen for detailed section measuring and sampling, and are referred to hereafter as the West and East Transects (the West Transect includes the W74 site on Eranondoo Hill). Each section was measured by tape resulting in cm-scale accuracy for the stratigraphic columns and relative sample positions. The West Transect is oriented northwest–southeast, and the East Transect is roughly north–south. GPS readings were obtained at positions along each transect and for certain samples in between (Appendix A), but due to the larger uncertainty of GPS readings, the relative distances measured by tape are more precise. For determining distances outside of the transects, GPS readings in d.m.s. were converted to UTM coordinates (Zone 50J) using the WGS 1984 datum. Both transects occur within the 220 m conglomerate-bearing section described in Wilde and Pidgeon (1990), and their younging directions were determined from preserved sedimentary features such as cross-bedding and graded bedding. The two transects are comprised of chemically mature sediments, including conglomerate, quartzite, and sandstone and are remarkably quartz-rich (average values of SiO_2 >95%, Al_2O_3 <3.0%, and K_2O <1.0%, Table 1). Hand-sample descriptions, mineralogy, and locations are listed in Appendix A. All individual zircons discussed below have the prefix 01JH, as in Table 2, which is omitted henceforth. For example, the grain 01JH54-34 is referenced as 54-34, which refers to sample number (01JH54) and grain number (34).

4. Analytical methods

4.1. Sample preparation

Two different methods were used to separate zircons from their host rocks. Conventional jaw crushing and disc milling were used to reduce all of the samples except 01JH36 and 01JH54 to sand-size particles. Zircons were then concentrated using heavy liquids, a Frantz magnetic separator, and finally by hand picking. After several samples were processed using the conventional method, it became clear that many of the zircons were angular broken fragments. To avoid mechanically shattering the zircons during processing, the Electric Pulse Disaggregation (EPD) method (Weiblen, 1994; Rudashevsky et al., 1995) was chosen for samples 01JH36 and 01JH54. EPD is an alternative method for disaggregating a rock that avoids crushing and grinding. High voltage electrical discharges (>100 kV) through a water bath that contains a sample are used to reduce a crystalline rock to sand-sized particles. This technique results in a sample that is largely disaggregated along, rather than across, grain boundaries and is particularly useful for liberating intact accessory minerals (Weiblen, 1994). After EPD, zircons from the two samples were concentrated in the same manner as the other samples. All zircon mounts were prepared as 1″ round epoxy mounts, polished using ~0.05 μm grit, and contained 100–500 grains each. Several of our mounts (W74, 01JH43, −47, −60, −63, −65, −113) contain zircons cast in random orientations. Zircons from the two EPD-separated samples (01JH36, 01JH54), and 01JH42, were specifically cast with their polished surfaces parallel to their crystallographic *C*-axes.

4.2. Electron beam and X-ray analysis

The zircon mounts were imaged by CL, BSE, and reflected light for use during ion probe navigation. After the SHRIMP (Sensitive High mass Resolution Ion Micro-Probe) analytical sessions, a second set of images was taken of the zircons in order to characterize the ion probe analysis locations. BSE and CL imaging was done with a Cameca SX51 electron microprobe (20 kV and 10 nA), and a LEO 1550 Scanning Electron Microscope (SEM) (5 kV, 1 nA), both at the University of Wisconsin, and a Phillips SX30 SEM (12 kV,

Table 1
X-ray fluorescence (XRF) whole-rock analyses of Jack Hills metasediments

Sample	Rock type	SiO_2 (wt.%) (0.01)[a]	Al_2O_3 (wt.%) (0.01)[a]	CaO (wt.%) (0.01)[a]	MgO (wt.%) (0.01)[a]	Na_2O (wt.%) (0.01)[a]	K_2O (wt.%) (0.01)[a]	Fe_2O_3 (wt.%) (0.01)[a]	MnO (wt.%) (0.01)[a]	TiO_2 (wt.%) (0.01)[a]	P_2O_5 (wt.%) (0.01)[a]	Cr_2O_3 (wt.%) (0.01)[a]	LOI (wt.%) (0.01)[a]	Total (wt.%)	Rb (ppm) (2)[a]	Sr (ppm) (2)[a]	Y (ppm) (2)[a]	Zr (ppm) (2)[a]	Nb (ppm) (2)[a]	Ba (ppm) (20)[a]
West Transect																				
01JH-63	Q	97.70	1.33	bd	0.06	0.04	0.35	0.23	0.04	0.09	bd	bd	0.15	100.0	22	2	bd	42	bd	78
01JH-62	S	92.53	4.09	bd	0.11	0.04	1.06	1.12	bd	0.08	bd	bd	1.10	100.1	31	11	bd	60	4	38
01JH-61	Q	96.40	0.82	0.04	0.06	0.03	0.03	1.64	bd	0.02	bd	bd	0.90	100.0	14	bd	bd	54	2	213
01JH-60	C	92.20	4.21	bd	0.13	0.05	1.02	0.93	bd	0.26	0.02	0.07	1.10	100.1	40	13	55	481	13	197
01JH-59	S	94.38	3.37	bd	0.10	0.05	0.89	0.52	bd	0.04	bd	bd	0.75	100.1	24	8	2	52	2	61
01JH-54	C	94.90	2.28	bd	0.11	0.05	0.67	1.02	bd	0.23	0.04	0.18	0.57	100.1	32	8	45	318	18	44
01JH-55	C	94.90	2.61	bd	0.10	0.05	0.74	0.74	bd	0.17	0.03	0.09	0.65	100.1	34	9	35	200	13	50
01JH-64	Q/S	94.67	3.17	bd	0.13	0.03	0.87	0.17	bd	0.08	bd	bd	0.90	100.0	34	8	12	136	4	bd
01JH-65	Q	97.90	1.25	bd	0.06	0.03	0.32	0.13	bd	0.03	0.01	bd	0.05	100.0	25	9	3	60	3	30
East Transect																				
01JH-48	S	94.90	2.65	bd	0.06	0.01	0.09	0.74	bd	0.11	bd	bd	1.35	99.9	12	5	bd	67	bd	bd
01JH-47	C	97.30	1.56	bd	0.06	0.03	0.16	0.14	bd	0.1	bd	bd	0.70	100.0	18	4	bd	41	3	69
01JH-46	Q	96.24	2.20	0.03	0.06	bd	0.21	0.07	bd	0.14	bd	bd	1.05	100.0	17	4	bd	59	3	54
01JH-45	C	96.56	1.83	bd	0.10	0.02	0.50	0.36	0.01	0.16	bd	0.13	0.43	100.1	22	10	bd	60	5	36
01JH-44	Q	97.48	1.50	bd	0.08	0.02	0.41	0.07	bd	0.09	bd	bd	0.35	100.0	18	5	bd	45	2	bd
01JH-43	S	90.30	6.03	bd	0.14	0.09	1.72	0.20	bd	0.45	bd	0.01	1.10	100.1	55	9	17	99	6	73
01JH-42	C	96.40	2.16	bd	0.09	0.04	0.62	0.15	bd	0.18	bd	0.04	0.40	100.1	32	4	6	51	5	40
01JH-41	S	93.44	4.51	bd	0.06	0.06	1.20	0.13	bd	0.09	bd	0.05	0.90	100.5	35	15	5	129	4	33
01JH-40	C	95.00	2.89	bd	0.10	0.06	0.84	0.16	bd	0.14	bd	0.07	0.70	100.0	39	9	4	59	4	49
01JH-39	S	93.20	4.00	bd	0.08	0.05	0.99	0.48	0.03	0.13	0.01	0.32	0.92	100.3	33	25	12	147	6	48
01JH-49	S	93.97	3.95	bd	0.05	0.05	0.96	0.38	bd	0.09	bd	0.05	0.70	100.2	31	14	4	77	4	30
01JH-50	Q	96.42	2.30	bd	0.06	0.05	0.56	0.13	bd	0.06	bd	bd	0.50	100.1	22	17	bd	45	bd	bd
01JH-51	Q	97.82	1.34	bd	0.06	0.02	0.33	0.05	bd	0.05	bd	bd	0.30	100.0	14	6	bd	46	bd	bd
Other samples																				
01JH-36	Q	96.90	1.26	bd	0.08	0.03	0.22	0.60	0.01	0.09	bd	0.78	0.25	100.2	22	7	24	87	6	21
01JH-100	C	93.90	4.98	bd	0.01	0.05	0.28	0.16	bd	0.05	0.07	bd	0.57	100	19	28	7	69	4	64

For each transect, samples are arranged in the interpreted stratigraphic order (i.e. youngest on top), as in Fig. 6. bd: below detection; S: (meta)sandstone ($n = 7$); C: (meta)conglomerate ($n = 8$); Q: quartzite ($n = 9$).

[a] Detection limit.

Table 2
Zircon U–Th–Pb isotopic data from seven-cycle SHRIMP II analyses

Grain-spot	Run	Grain area[a]	U (ppm)	Th (ppm)	Th/U	Percentage comm. ^{206}Pb	$^{204}Pb/^{206}Pb$	$^{207}Pb^{b}/^{206}Pb^{b}$	$^{208}Pb^{b}/^{232}Th$	$^{208}Pb^{b}/^{206}Pb^{b}$	$^{206}Pb^{b}/^{238}U$	$^{207}Pb^{b}/^{235}U$	$^{207}Pb^{b}/^{206}Pb^{b}$ age (Ma)	Percentage concordance
Sample 01JH36 (Quartzite located between East and West transect; UTM: Easting = 499,947, Northing = 7,106,431; 226 grains analyzed, sixteen seven-cycle analyses)														
5-2	8	c	61	40	0.66	0.16	0.00008	0.33757 ± 0.00164	0.1942 ± 0.0068	0.1824 ± 0.0014	0.7334 ± 0.0248	34.14 ± 1.16	**3652 ± 7**	97
56-2	8	c	172	101	0.61	0.04	0.00002	0.32336 ± 0.00095	0.1676 ± 0.0056	0.1456 ± 0.0007	0.7027 ± 0.0233	31.33 ± 1.04	**3586 ± 5**	96
69-2	8	c	132	194	1.47	0.10	0.00005	0.49650 ± 0.00509	0.0592 ± 0.0023	0.1551 ± 0.0026	0.5850 ± 0.0199	40.04 ± 1.42	4231 ± 15	70[c]
69-3	8	c	95	71	0.75	0.14	0.00007	0.52890 ± 0.00658	0.1014 ± 0.0038	0.1045 ± 0.0015	0.7707 ± 0.0257	56.20 ± 2.00	**4324 ± 18**	85[c]
69-4	8	c	140	335	2.39	0.45	0.00024	0.40980 ± 0.00761	0.0248 ± 0.0011	0.1562 ± 0.0027	0.4149 ± 0.0150	23.44 ± 0.95	3946 ± 28	57[c]
69-5	8	c	244	473	1.94	1.57	0.00084	0.49680 ± 0.00551	0.0349 ± 0.0023	0.2114 ± 0.0106	0.3854 ± 0.0132	26.40 ± 0.95	4232 ± 16	50[c]
69-6	8	c	206	423	2.05	0.57	0.00030	0.44950 ± 0.00322	0.0310 ± 0.0012	0.1329 ± 0.0014	0.5391 ± 0.0184	33.41 ± 1.17	4084 ± 11	68[c]
69-7	8	r	125	252	2.02	1.20	0.00064	0.27980 ± 0.00354	0.0156 ± 0.0009	0.1350 ± 0.0033	0.2913 ± 0.0099	11.24 ± 0.41	3362 ± 20	49[c]
69-8	8	c/r	151	185	1.23	0.23	0.00012	0.48060 ± 0.00496	0.0853 ± 0.0030	0.1761 ± 0.0011	0.6282 ± 0.0214	41.63 ± 1.48	4183 ± 15	75[c]
69-9	8	c	159	201	1.26	0.36	0.00019	0.51960 ± 0.00503	0.0811 ± 0.0030	0.1704 ± 0.0020	0.6460 ± 0.0215	46.28 ± 1.61	4298 ± 14	75[c]
69-10	9	c/r	159	249	1.57	0.40	0.00021	0.34040 ± 0.00169	0.0309 ± 0.0010	0.1194 ± 0.0012	0.4463 ± 0.0119	20.94 ± 0.57	3664 ± 8	65[c]
69-11	9	c	79	47	0.59	0.24	0.00013	0.52410 ± 0.00321	0.1512 ± 0.0051	0.1384 ± 0.0022	0.7014 ± 0.0191	50.68 ± 1.42	4310 ± 9	80[c]
69-12	9	c	162	208	1.28	0.19	0.00010	0.52210 ± 0.00296	0.0901 ± 0.0027	0.1870 ± 0.0015	0.6542 ± 0.0187	47.09 ± 1.37	4305 ± 8	75[c]
86-2	8	u	378	87	0.23	0.02	0.00001	0.34404 ± 0.00064	0.1903 ± 0.0064	0.0619 ± 0.0003	0.7369 ± 0.0243	34.96 ± 1.15	**3681 ± 3**	97
115-2	8	c	176	51	0.29	0.09	0.00005	0.44400 ± 0.00447	0.1919 ± 0.0067	0.0770 ± 0.0006	0.7567 ± 0.0252	46.33 ± 1.61	**4065 ± 15**	89
140-2	9	u	48	156	3.27	1.56	0.00084	0.31816 ± 0.00963	0.0687 ± 0.0054	0.4940 ± 0.0342	0.4942 ± 0.0140	21.68 ± 0.90	3561 ± 47	73
Sample 01JH42 (Metaconglomerate from East Transect; UTM: Easting = 500,036, Northing = 7,106,455; 94 grains analyzed, three seven-cycle analyses)														
69b	7	c	176	58	0.33	0.00	0.00000	0.40308 ± 0.00161	0.1692 ± 0.0020	0.0829 ± 0.0008	0.6918 ± 0.0043	38.45 ± 0.28	3921 ± 6	86[c]
69d	7	c	306	112	0.37	0.00	0.00000	0.40830 ± 0.00122	0.1724 ± 0.0014	0.0955 ± 0.0006	0.6842 ± 0.0034	38.52 ± 0.22	**3940 ± 4**	85
75b	7	u	217	66	0.30	0.13	0.00007	0.41039 ± 0.00246	0.1290 ± 0.0028	0.0771 ± 0.0012	0.5471 ± 0.0047	30.96 ± 0.33	3948 ± 9	71[c]
Sample 01JH47 (Metaconglomerate from East Transect; located 4.0 m south of 01JH42; 70 grains analyzed, three seven-cycle analyses)														
33-2	1	c	340	665	1.96	0.84	0.00045	0.41255 ± 0.00124	0.0085 ± 0.0006	0.0486 ± 0.0005	0.5430 ± 0.0103	30.89 ± 0.59	3955 ± 4	71[c]
b-2-2	2	u	218	154	0.71	0.13	0.00007	0.18797 ± 0.00081	0.0565 ± 0.0013	0.0935 ± 0.0006	0.4522 ± 0.0084	11.72 ± 0.22	**2724 ± 7**	88
b-3-2	2	u	502	552	1.10	0.20	0.00011	0.16462 ± 0.00060	0.0587 ± 0.0012	0.1558 ± 0.0009	0.4387 ± 0.0080	9.96 ± 0.19	**2504 ± 6**	94
Sample 01JH54 (Metaconglomerate from West Transect; UTM: Easting = 499,137, Northing = 7,105,849; 146 grains analyzed, 64 seven-cycle analyses)														
10-2	3	c	123	128	1.04	0.00	0.00000	0.45952 ± 0.00120	0.2262 ± 0.0023	0.2742 ± 0.0011	0.8839 ± 0.0082	56.00 ± 0.54	4116 ± 4	99
10-3	3	c	58	55	0.94	0.00	0.00000	0.45891 ± 0.00180	0.1921 ± 0.0020	0.2215 ± 0.0014	0.8410 ± 0.0070	53.22 ± 0.49	4114 ± 6	96
10-4	3	c	85	69	0.82	0.00	0.00000	0.46153 ± 0.00149	0.2252 ± 0.0021	0.2129 ± 0.0011	0.8895 ± 0.0063	56.61 ± 0.44	**4123 ± 5**	100
17-2	3	c	199	62	0.31	0.02	0.00001	0.47912 ± 0.00199	0.2207 ± 0.0020	0.0804 ± 0.0005	0.8929 ± 0.0042	58.99 ± 0.37	**4178 ± 6**	98
17-3	3	c	392	224	0.57	0.08	0.00004	0.47247 ± 0.00160	0.1621 ± 0.0010	0.1129 ± 0.0005	0.8581 ± 0.0030	55.90 ± 0.27	4158 ± 5	96
17-4	3	c	400	186	0.46	0.07	0.00004	0.41695 ± 0.00159	0.1657 ± 0.0010	0.1054 ± 0.0004	0.7640 ± 0.0027	43.92 ± 0.23	3971 ± 6	92
17-5	3	r	276	248	0.90	0.18	0.00010	0.45581 ± 0.00219	0.0884 ± 0.0008	0.1146 ± 0.0005	0.7370 ± 0.0031	46.32 ± 0.30	4104 ± 7	87
17-6	3	c	383	178	0.46	0.03	0.00002	0.46861 ± 0.00085	0.1831 ± 0.0012	0.1184 ± 0.0006	0.7452 ± 0.0029	48.15 ± 0.21	4145 ± 3	87
20-2	3	c	179	88	0.49	0.05	0.00002	0.45754 ± 0.00099	0.2226 ± 0.0016	0.1285 ± 0.0006	0.8836 ± 0.0042	55.74 ± 0.29	**4110 ± 3**	99
20-3	3	r	152	172	1.13	0.11	0.00006	0.44956 ± 0.00221	0.0601 ± 0.0007	0.0919 ± 0.0005	0.7827 ± 0.0041	48.52 ± 0.35	4084 ± 7	91
34-2	4	c	164	60	0.37	0.08	0.00004	0.47477 ± 0.00189	0.2271 ± 0.0133	0.0962 ± 0.0006	0.9125 ± 0.0533	59.74 ± 3.49	**4165 ± 6**	100
34-3	4	c	259	113	0.43	0.13	0.00007	0.47552 ± 0.00164	0.1526 ± 0.0090	0.0827 ± 0.0006	0.8555 ± 0.0499	56.09 ± 3.28	4167 ± 5	96
37-2	4	r	128	38	0.29	0.11	0.00006	0.37129 ± 0.00170	0.2000 ± 0.0120	0.0770 ± 0.0006	0.8141 ± 0.0476	41.68 ± 2.44	3797 ± 7	101
37-3	9	c	218	113	0.52	0.03	0.00002	0.39871 ± 0.00083	0.2099 ± 0.0056	0.1392 ± 0.0005	0.8101 ± 0.0213	44.54 ± 1.17	**3904 ± 3**	98
40-2	4	c	117	84	0.72	0.06	0.00003	0.44790 ± 0.00144	0.2266 ± 0.0133	0.1879 ± 0.0010	0.9015 ± 0.0527	55.67 ± 3.26	**4078 ± 5**	102
58-2	4	c	118	99	0.84	0.19	0.00010	0.43540 ± 0.00142	0.2278 ± 0.0135	0.2253 ± 0.0011	0.8934 ± 0.0526	53.64 ± 3.16	4036 ± 5	102
58-3	4	c	87	68	0.79	0.23	0.00012	0.44321 ± 0.00221	0.2250 ± 0.0135	0.2052 ± 0.0019	0.9089 ± 0.0534	55.54 ± 3.28	**4063 ± 7**	103
66-2	4	c	166	59	0.35	0.16	0.00009	0.48448 ± 0.00128	0.2217 ± 0.0132	0.0921 ± 0.0006	0.9146 ± 0.0535	61.10 ± 3.58	**4195 ± 4**	100

66-3	4	r	88	46	0.53	0.43	0.00023	0.47645 ± 0.00187	0.2069 ± 0.0126	0.1395 ± 0.0010	0.8641 ± 0.0511	56.77 ± 3.37	4170 ± 6	96
66-4	4	r	139	51	0.37	0.18	0.00009	0.46924 ± 0.00426	0.2253 ± 0.0140	0.0989 ± 0.0009	0.8934 ± 0.0543	57.80 ± 3.55	4147 ± 13	99
66-R1	6	r	230	441	1.92	0.97	0.00052	0.42784 ± 0.00198	0.0101 ± 0.0005	0.0893 ± 0.0011	0.2868 ± 0.0071	16.76 ± 0.42	3996 ± 7	41[c]
66-R2	6	r	109	41	0.38	0.14	0.00008	0.47259 ± 0.00266	0.2072 ± 0.0057	0.1012 ± 0.0011	0.8267 ± 0.0200	53.81 ± 1.34	4156 ± 8	93
68-2	4	r	154	242	1.57	0.32	0.00017	0.47283 ± 0.00142	0.0896 ± 0.0053	0.1813 ± 0.0009	0.8295 ± 0.0485	54.08 ± 3.16	4159 ± 4	94
68-3	4	r	121	77	0.64	0.10	0.00005	0.47842 ± 0.00151	0.2149 ± 0.0127	0.1655 ± 0.0010	0.8659 ± 0.0507	57.12 ± 3.35	**4176 ± 5**	96
68-R3	6	r	127	188	1.48	0.37	0.00020	0.47195 ± 0.00127	0.0824 ± 0.0023	0.1737 ± 0.0013	0.7561 ± 0.0191	49.20 ± 1.25	4156 ± 4	87
77-1	4	c	73	40	0.55	0.61	0.00032	0.47400 ± 0.00426	0.2041 ± 0.0135	0.1476 ± 0.0013	0.8491 ± 0.0535	55.50 ± 3.55	4162 ± 13	95
77-2	4	c/r	217	55	0.25	0.17	0.00009	0.34290 ± 0.00137	0.1812 ± 0.0116	0.0681 ± 0.0005	0.7257 ± 0.0450	34.31 ± 2.13	3676 ± 7	96
77-3	4	c/r	350	406	1.16	0.49	0.00026	0.33600 ± 0.00168	0.0221 ± 0.0015	0.0605 ± 0.0004	0.5229 ± 0.0324	24.23 ± 1.50	3645 ± 7	74[c]
77-4	4	c	147	112	0.76	0.13	0.00006	0.52870 ± 0.00211	0.2430 ± 0.0153	0.1996 ± 0.0010	0.9724 ± 0.0603	70.90 ± 4.40	**4324 ± 6**	101
77-5	4	c/r	161	206	1.28	0.31	0.00017	0.43450 ± 0.00130	0.0702 ± 0.0044	0.1395 ± 0.0008	0.6955 ± 0.0431	41.66 ± 2.58	4033 ± 5	84[c]
77-6	4	c	69	41	0.59	0.36	0.00019	0.50650 ± 0.00253	0.1409 ± 0.0093	0.1206 ± 0.0012	0.7643 ± 0.0474	53.37 ± 3.36	4260 ± 7	86
77-7	4	c	122	125	1.02	0.31	0.00016	0.51400 ± 0.00205	0.1254 ± 0.0079	0.1668 ± 0.0010	0.8240 ± 0.0511	58.39 ± 3.62	4282 ± 5	90
77-8	5	c	106	100	0.94	1.39	0.00074	0.41090 ± 0.00534	0.1086 ± 0.0070	0.1585 ± 0.0036	0.8059 ± 0.0210	45.66 ± 1.32	3950 ± 20	96
77-9	5	c	113	129	1.14	1.77	0.00095	0.50030 ± 0.00350	0.0900 ± 0.0062	0.1744 ± 0.0047	0.7606 ± 0.0198	52.47 ± 1.42	4242 ± 10	86
77-10	5	c	169	242	1.43	0.68	0.00036	0.50640 ± 0.00202	0.0892 ± 0.0032	0.1806 ± 0.0033	0.7846 ± 0.0196	54.79 ± 1.42	4260 ± 6	88
77-11	5	c	142	99	0.70	0.97	0.00052	0.47980 ± 0.00239	0.2212 ± 0.0077	0.1944 ± 0.0016	0.8994 ± 0.0225	59.51 ± 1.55	4180 ± 7	99
77-12	5	c/r	304	247	0.81	1.28	0.00068	0.34220 ± 0.00205	0.0290 ± 0.0024	0.0692 ± 0.0012	0.5619 ± 0.0140	26.51 ± 0.69	3673 ± 10	78[c]
77-13	5	c/r	186	45	0.24	0.81	0.00043	0.35100 ± 0.00245	0.1873 ± 0.0139	0.0795 ± 0.0026	0.7438 ± 0.0208	36.00 ± 1.04	3711 ± 10	97
77-14	5	c	73	33	0.45	1.61	0.00086	0.50790 ± 0.00355	0.2238 ± 0.0233	0.1406 ± 0.0048	0.9437 ± 0.0255	66.08 ± 1.85	4264 ± 10	100
78-2	8	c	198	77	0.39	0.07	0.00004	0.47537 ± 0.00145	0.2199 ± 0.0076	0.1045 ± 0.0009	0.8535 ± 0.0283	55.94 ± 1.86	**4167 ± 5**	95
78-3	8	r	90	37	0.41	0.35	0.00019	0.27989 ± 0.00177	0.1127 ± 0.0049	0.0839 ± 0.0011	0.6201 ± 0.0210	23.93 ± 0.83	3362 ± 10	93
78-4	8	r	111	45	0.40	0.12	0.00006	0.43831 ± 0.00166	0.1840 ± 0.0067	0.1004 ± 0.0008	0.7779 ± 0.0261	47.01 ± 1.58	4046 ± 6	92
78-5	8	c	205	93	0.45	0.01	0.00001	0.46538 ± 0.00188	0.2271 ± 0.0077	0.1203 ± 0.0007	0.8845 ± 0.0294	56.75 ± 1.90	4135 ± 6	99
78-6	9	r	272	529	1.95	0.56	0.00030	0.33796 ± 0.00262	0.0112 ± 0.0005	0.1176 ± 0.0031	0.2112 ± 0.0058	9.84 ± 0.28	3654 ± 12	34[c]
81-2	8	c	170	72	0.42	0.06	0.00003	0.45399 ± 0.00162	0.2184 ± 0.0075	0.1129 ± 0.0007	0.8511 ± 0.0284	53.28 ± 1.79	4098 ± 5	97
81-3	8	c	138	60	0.43	0.17	0.00009	0.45539 ± 0.00166	0.2103 ± 0.0076	0.1160 ± 0.0013	0.8350 ± 0.0280	52.43 ± 1.77	**4103 ± 5**	95
81-4	8	r	201	12	0.06	0.13	0.00007	0.33693 ± 0.00119	0.1115 ± 0.0088	0.0135 ± 0.0004	0.6637 ± 0.0221	30.84 ± 1.03	3649 ± 5	90
81-5	9	r	409	681	1.66	4.86	0.00260	0.37987 ± 0.00639	0.0055 ± 0.0009	0.1879 ± 0.0027	0.1027 ± 0.0028	5.38 ± 0.17	3831 ± 25	16[c]
90-2	4	c	296	404	1.36	0.17	0.00009	0.50750 ± 0.00130	0.1106 ± 0.0065	0.2015 ± 0.0018	0.7859 ± 0.0458	54.99 ± 3.21	**4263 ± 4**	88[c]
90-3	4	r	672	679	1.01	0.40	0.00021	0.46302 ± 0.00112	0.0249 ± 0.0015	0.0806 ± 0.0008	0.3568 ± 0.0208	22.78 ± 1.33	4128 ± 4	48[c]
90-X	6	c	320	576	1.80	0.62	0.00033	0.50423 ± 0.00128	0.0282 ± 0.0008	0.1630 ± 0.0015	0.3458 ± 0.0085	24.04 ± 0.60	4254 ± 4	45[c]
90-1	9	r	165	113	0.69	0.87	0.00047	0.42107 ± 0.00262	0.0356 ± 0.0017	0.0916 ± 0.0014	0.3410 ± 0.0095	19.80 ± 0.57	3986 ± 9	47[c]
90-2	9	c/r	333	176	0.53	0.15	0.00008	0.45812 ± 0.00228	0.0634 ± 0.0019	0.0583 ± 0.0004	0.6263 ± 0.0164	39.56 ± 1.05	4112 ± 7	76[c]
90-3	9	c	630	1028	1.63	2.54	0.00136	0.39471 ± 0.00321	0.0072 ± 0.0007	0.1334 ± 0.0037	0.1452 ± 0.0039	7.90 ± 0.22	3889 ± 12	22[c]

Table 2 (*Continued*)

Grain-spot	Run	Grain area[a]	U (ppm)	Th (ppm)	Th/U	Percentage comm. ^{206}Pb	$^{204}Pb/^{206}Pb$	$^{207}Pb^{b}/^{206}Pb^{b}$	$^{208}Pb^{b}/^{232}Th$	$^{208}Pb^{b}/^{206}Pb^{b}$	$^{206}Pb^{b}/^{238}U$	$^{207}Pb^{b}/^{235}U$	$^{207}Pb^{b}/^{206}Pb^{b}$ age (Ma)	Percentage concordance
90-4	9	c	304	396	1.30	0.13	0.00007	0.50352 ± 0.00083	0.1303 ± 0.0035	0.2296 ± 0.0006	0.7721 ± 0.0205	53.61 ± 1.43	4252 ± 2	87[c]
90-5	9	r	101	64	0.64	0.53	0.00028	0.43352 ± 0.00175	0.0661 ± 0.0029	0.0727 ± 0.0007	0.6997 ± 0.0189	41.82 ± 1.14	4030 ± 6	85
D2-X	6	c	344	285	0.83	0.37	0.00020	0.44830 ± 0.00097	0.0735 ± 0.0019	0.1380 ± 0.0008	0.4797 ± 0.0112	29.65 ± 0.69	4080 ± 3	62[c]
D2	9	c	189	142	0.75	0.10	0.00005	0.43705 ± 0.00150	0.1641 ± 0.0046	0.1620 ± 0.0009	0.7984 ± 0.0214	48.11 ± 1.30	**4042 ± 5**	94
D7-X	6	c	372	309	0.83	0.53	0.00029	0.51724 ± 0.00142	0.0756 ± 0.0020	0.1984 ± 0.0012	0.3440 ± 0.0086	24.53 ± 0.62	4291 ± 4	44[c]
D7-2	8	c	507	887	1.75	0.29	0.00016	0.51764 ± 0.00152	0.0323 ± 0.0011	0.1832 ± 0.0009	0.3289 ± 0.0109	23.47 ± 0.78	4292 ± 4	43[c]
D7-3	8	c	275	173	0.63	0.07	0.00003	0.53765 ± 0.00119	0.1985 ± 0.0066	0.1472 ± 0.0007	0.8859 ± 0.0293	65.67 ± 2.18	**4348 ± 3**	94
D7-4	8	c	327	569	1.74	0.27	0.00014	0.49911 ± 0.00137	0.0373 ± 0.0013	0.1397 ± 0.0008	0.4990 ± 0.0171	34.34 ± 1.18	4239 ± 4	62[c]
D7-5	8	c	526	1011	1.92	0.34	0.00018	0.49940 ± 0.00155	0.0218 ± 0.0008	0.1709 ± 0.0009	0.2633 ± 0.0088	18.13 ± 0.61	4239 ± 5	36[c]
D7-6	9	c	489	648	1.33	0.07	0.00004	0.45257 ± 0.00085	0.0309 ± 0.0010	0.0798 ± 0.0016	0.5398 ± 0.0141	33.69 ± 0.88	4094 ± 3	68[c]
Sample 01JH60 (Metaconglomerate from West Transect; 25 m southwest of the W74/01JH54 site; 100 grains analyzed, 15 seven-cycle analyses)														
39-2	1	c	89	43	0.48	0.07	0.00004	0.47865 ± 0.00585	0.2252 ± 0.0048	0.1244 ± 0.0008	0.9086 ± 0.0178	59.97 ± 1.38	**4177 ± 18**	100
39-3	1	r	194	68	0.35	0.37	0.00020	0.39918 ± 0.00121	0.0439 ± 0.0039	0.0290 ± 0.0007	0.7461 ± 0.0141	41.06 ± 0.78	3906 ± 5	92
47-2	1	c	133	173	1.30	0.38	0.00020	0.42503 ± 0.00264	0.0437 ± 0.0013	0.1010 ± 0.0014	0.6313 ± 0.0121	37.00 ± 0.75	4000 ± 9	79
47-3	1	c	232	562	2.42	1.59	0.00085	0.43590 ± 0.00210	0.0151 ± 0.0009	0.1021 ± 0.0016	0.5363 ± 0.0105	32.23 ± 0.65	4038 ± 7	69[c]
51-2	1	c	35	11	0.31	0.01	0.00000	0.45935 ± 0.00239	0.2410 ± 0.0067	0.0866 ± 0.0011	0.8922 ± 0.0192	56.50 ± 1.25	**4116 ± 8**	100
51-3	1	c	42	13	0.31	0.14	0.00008	0.44103 ± 0.00636	0.2276 ± 0.0073	0.0885 ± 0.0015	0.8782 ± 0.0209	53.40 ± 1.49	4055 ± 21	100
56-2	1	c	429	474	1.10	0.87	0.00047	0.44865 ± 0.00180	0.0401 ± 0.0012	0.1032 ± 0.0004	0.5326 ± 0.0101	32.95 ± 0.64	4081 ± 6	67[c]
64-2	1	c	54	40	0.74	0.09	0.00005	0.43646 ± 0.00188	0.2254 ± 0.0050	0.1963 ± 0.0014	0.8869 ± 0.0181	53.37 ± 1.11	**4040 ± 6**	101
64-4	1	r	2787	20956	7.52	49.06	0.02623	0.27570 ± 0.10126	-	1.0735 ± 0.0260	0.0383 ± 0.0022	1.46 ± 0.54	3339 ± 575	7[c]
68-3	1	c	174	48	0.27	1.17	0.00063	0.45355 ± 0.00393	0.1356 ± 0.0146	0.0710 ± 0.0033	0.8080 ± 0.0152	50.53 ± 1.05	**4097 ± 13**	93
68-4	1	r	91	52	0.56	0.33	0.00017	0.43251 ± 0.00170	0.1220 ± 0.0037	0.0952 ± 0.0012	0.8025 ± 0.0171	47.86 ± 1.04	4026 ± 6	94[cc]
83-2	1	r	212	566	2.67	5.12	0.00274	0.40228 ± 0.00644	0.0158 ± 0.0013	0.2560 ± 0.0028	0.2744 ± 0.0054	15.22 ± 0.38	3918 ± 24	40[c]
83-3	1	c	2822	3405	1.21	52.49	0.02806	0.34662 ± 0.11492	-	1.1412 ± 0.0160	0.0467 ± 0.0467	2.23 ± 0.75	3692 ± 506	8[c]
85-2	2	c	90	127	1.41	8.17	0.00437	0.39427 ± 0.00975	0.0310 ± 0.0056	0.2740 ± 0.0115	0.3952 ± 0.0103	21.48 ± 0.77	3887 ± 37	55[c]
87-2	2	c	789	1360	1.72	1.51	0.00081	0.39317 ± 0.00209	0.0105 ± 0.0016	0.0732 ± 0.0039	0.4381 ± 0.0102	23.75 ± 0.57	3883 ± 8	60[c]
Sample 01JH63 (Quartzite from West Transect; UTM: Easting = 499,153, Northing = 7,105,794; 58 grains analyzed, eight seven-cycle analyses)														
1-2	2	c	215	214	0.99	0.02	0.00001	0.18929 ± 0.00068	0.1451 ± 0.0028	0.2792 ± 0.0011	0.5338 ± 0.0100	13.93 ± 0.27	**2736 ± 6**	101
7-2	2	u	326	99	0.30	0.21	0.00011	0.12115 ± 0.00078	0.1007 ± 0.0023	0.0902 ± 0.0006	0.3686 ± 0.0068	6.16 ± 0.12	**1973 ± 11**	103
23-2	2	c	117	75	0.64	0.29	0.00015	0.09747 ± 0.00117	0.0824 ± 0.0020	0.1994 ± 0.0018	0.2802 ± 0.0055	3.77 ± 0.09	**1576 ± 22**	101
27-2	2	c	247	100	0.40	0.14	0.00008	0.17642 ± 0.00110	0.1301 ± 0.0027	0.1144 ± 0.0007	0.4846 ± 0.0090	11.79 ± 0.23	**2620 ± 10**	97[c]
27-3	2	c	560	106	0.19	15.97	0.00854	0.15956 ± 0.02040	0.0747 ± 0.0729	0.3631 ± 0.0041	0.3680 ± 0.0078	8.10 ± 1.05	2451 ± 216	82[c]
31-2	2	c	594	231	0.39	2.25	0.00120	0.17298 ± 0.00316	0.1003 ± 0.0070	0.1532 ± 0.0034	0.3699 ± 0.0068	8.82 ± 0.23	2587 ± 30	78[c]
36-2	2	c	436	500	1.15	2.65	0.00141	0.17329 ± 0.00313	0.0733 ± 0.0027	0.2457 ± 0.0009	0.4428 ± 0.0082	10.58 ± 0.27	**2590 ± 30**	91
53-2	2	c	411	185	0.45	0.86	0.00046	0.10716 ± 0.00128	0.0840 ± 0.0025	0.1582 ± 0.0023	0.2759 ± 0.0051	4.08 ± 0.09	**1752 ± 22**	90
Sample 01JH65 (Quartzite from West Transect; UTM: Easting = 499,109, Northing = 7,105,840; 46 grains analyzed, one seven-cycle analysis)														
22-2	2	u	181	8	0.04	0.03	0.00002	0.44290 ± 0.00283	0.1993 ± 0.0089	0.0113 ± 0.0002	0.8483 ± 0.0212	51.81 ± 1.34	**4062 ± 10**	98
Sample W74/3 (Metaconglomerate from West Transect; location published in Compston and Pidgeon (1986); 173 grains analyzed, 30 seven-cycle analyses)														
7-2	9	c	150	65	0.43	0.08	0.00004	0.44788 ± 0.00142	0.2166 ± 0.0062	0.1141 ± 0.0008	0.8620 ± 0.0230	53.23 ± 1.43	**4078 ± 5**	98
13-2	9	u	310	239	0.77	0.04	0.00002	0.42743 ± 0.00146	0.2137 ± 0.0057	0.2065 ± 0.0009	0.8289 ± 0.0217	48.85 ± 1.29	**4008 ± 5**	97
15-2	9	c	70	13	0.19	0.15	0.00008	0.43000 ± 0.00401	0.2047 ± 0.0078	0.0504 ± 0.0006	0.8280 ± 0.0224	49.09 ± 1.41	**4017 ± 14**	97
17-2	9	c	192	118	0.61	0.28	0.00015	0.42870 ± 0.00112	0.0993 ± 0.0029	0.0977 ± 0.0006	0.6836 ± 0.0180	40.41 ± 1.07	4013 ± 4	84[c]

30-2	9	u	117	59	0.50	0.26	0.00014	0.42855 ± 0.00134	0.1797 ± 0.0052	0.1266 ± 0.0008	0.7710 ± 0.0205	45.56 ± 1.22	4012 ± 5	92
30-3	9	u	121	49	0.41	0.13	0.00007	0.45524 ± 0.00670	0.1979 ± 0.0061	0.1053 ± 0.0012	0.8075 ± 0.0221	50.69 ± 1.57	**4102 ± 22**	93
32-2	9	u	297	472	1.59	0.53	0.00029	0.45181 ± 0.00125	0.0357 ± 0.0011	0.1255 ± 0.0006	0.5097 ± 0.0135	31.75 ± 0.85	4091 ± 4	65[c]
36-2	9	u	139	46	0.33	0.12	0.00006	0.41496 ± 0.00205	0.1897 ± 0.0060	0.0853 ± 0.0011	0.7810 ± 0.0217	44.69 ± 1.26	**3964 ± 7**	94
36-3	9	u	129	42	0.32	0.13	0.00007	0.41213 ± 0.00334	0.1729 ± 0.0051	0.0835 ± 0.0007	0.7120 ± 0.0193	40.46 ± 1.14	3954 ± 12	88
41-2	9	c	67	43	0.64	0.11	0.00006	0.45820 ± 0.00177	0.2152 ± 0.0065	0.1691 ± 0.0013	0.8504 ± 0.0242	53.72 ± 1.54	**4112 ± 6**	96
58-2	9	u	142	75	0.53	0.07	0.00004	0.43797 ± 0.00131	0.1951 ± 0.0054	0.1403 ± 0.0008	0.7663 ± 0.0203	46.28 ± 1.24	**4045 ± 4**	91
62-2	9	c	255	72	0.28	0.08	0.00004	0.46463 ± 0.00184	0.1741 ± 0.0054	0.0700 ± 0.0011	0.7454 ± 0.0197	47.75 ± 1.28	**4133 ± 6**	87
74-2	9	u	175	155	0.89	0.34	0.00018	0.43500 ± 0.00333	0.0553 ± 0.0018	0.0884 ± 0.0013	0.6202 ± 0.0164	37.20 ± 1.02	4035 ± 11	77[c]
114-2	9	c	211	70	0.33	0.10	0.00005	0.43283 ± 0.00146	0.1266 ± 0.0039	0.0567 ± 0.0006	0.7981 ± 0.0218	47.63 ± 1.31	**4027 ± 5**	94
127-2	9	c	191	166	0.87	0.04	0.00002	0.41404 ± 0.00119	0.2154 ± 0.0057	0.2319 ± 0.0009	0.8369 ± 0.0221	47.78 ± 1.27	3961 ± 4	99
127-3	9	c	211	187	0.88	0.04	0.00002	0.42887 ± 0.00097	0.2223 ± 0.0059	0.2364 ± 0.0008	0.8610 ± 0.0227	50.92 ± 1.35	**4014 ± 3**	100
131-2	10	u	451	91	0.20	0.02	0.00001	0.46367 ± 0.00217	0.2134 ± 0.0061	0.0528 ± 0.0003	0.8459 ± 0.0233	54.08 ± 1.51	**4130 ± 7**	96
131-3	10	u	1958	1922	0.98	5.18	0.00277	0.35828 ± 0.00917	0.0085 ± 0.0035	0.1813 ± 0.0004	0.1094 ± 0.0121	5.40 ± 0.61	3743 ± 39	18[c]
131-4	10	u	521	100	0.19	0.08	0.00004	0.45602 ± 0.00169	0.1983 ± 0.0059	0.0490 ± 0.0004	0.8271 ± 0.0228	52.01 ± 1.45	4105 ± 6	95[c]
133-2	10	c	95	36	0.38	0.26	0.00014	0.42397 ± 0.00181	0.1946 ± 0.0065	0.1018 ± 0.0009	0.7861 ± 0.0224	45.95 ± 1.32	**3996 ± 6**	94
134-2	10	c	147	139	0.95	0.42	0.00022	0.41101 ± 0.00220	0.0793 ± 0.0028	0.1240 ± 0.0009	0.6692 ± 0.0192	37.92 ± 1.11	3950 ± 8	84
134-3	10	c	101	52	0.52	0.24	0.00013	0.42049 ± 0.00178	0.2033 ± 0.0064	0.1403 ± 0.0011	0.8043 ± 0.0229	46.63 ± 1.35	**3984 ± 6**	96
143-2	10	c	101	26	0.26	0.07	0.00004	0.47291 ± 0.00380	0.2007 ± 0.0069	0.0600 ± 0.0007	0.9161 ± 0.0260	59.74 ± 1.77	**4159 ± 12**	101
152-2	10	c	122	56	0.46	0.10	0.00005	0.43340 ± 0.00168	0.2044 ± 0.0063	0.1197 ± 0.0010	0.8174 ± 0.0231	48.85 ± 1.39	**4029 ± 6**	96
154-1	10	c	61	18	0.30	0.22	0.00012	0.47468 ± 0.01056	0.2060 ± 0.0097	0.0790 ± 0.0016	0.8478 ± 0.0248	55.49 ± 2.04	**4164 ± 33**	95
154-2	10	r	59	18	0.30	0.38	0.00020	0.44706 ± 0.00252	0.1975 ± 0.0109	0.0784 ± 0.0011	0.8601 ± 0.0253	53.02 ± 1.59	4075 ± 8	98
160-2	10	c	524	133	0.25	0.20	0.00011	0.20511 ± 0.00067	0.1176 ± 0.0035	0.0746 ± 0.0004	0.4359 ± 0.0120	12.33 ± 0.34	2867 ± 5	81
170-2	10	c	89	28	0.31	0.27	0.00014	0.44503 ± 0.00202	0.1802 ± 0.0063	0.0848 ± 0.0009	0.7374 ± 0.0210	45.25 ± 1.31	**4069 ± 7**	88
174-2	10	c	134	99	0.74	0.11	0.00006	0.45273 ± 0.00198	0.2242 ± 0.0065	0.1984 ± 0.0011	0.8754 ± 0.0247	54.64 ± 1.56	**4094 ± 7**	99
174-3	10	c	147	92	0.63	0.02	0.00001	0.44760 ± 0.00158	0.2211 ± 0.0063	0.1598 ± 0.0009	0.8961 ± 0.0252	55.30 ± 1.57	4077 ± 5	101

All errors are 1σ. comm: common; percentage concordance (conc.) = [(^{206}Pb/^{238}U age)/(^{207}Pb/^{206}Pb age)] × 100. Age in Ma. UTM: Universal Transverse Mercator. Bolded ^{207}Pb/^{206}Pb ages indicate preferred core age of grain (see text for criteria).

[a] Grain area as interpreted from CL images; c: core, r: rim, u: unknown.

[b] A ^{204}Pb corrected Pb value (Ludwig, 2001b).

[c] Analysis where SHRIMP spot was later found to be located on a visible crack by optical microscopy, BSE, or CL.

and ∼20 nA) at Curtin University. The ability to interpret CL images was largely a function of the crystallographic orientation of the mounted grain and the extent to which the polished surface exposed the grain interior. CL structures in zircons that were individually mounted with the *C*-axis parallel to the polished surface (samples 01JH36, 01JH42, and 01JH54) are generally unambiguous, i.e. core and rim domains and fine zoning patterns were easily discernable. Furthermore, since the zircons were placed on a flat surface for mounting, subsequent grinding and polishing exposed the cores of all grains that were of similar size. In contrast, randomly oriented zircons yielded CL patterns that are often ambiguous; the depth of the exposed cross-section for each crystal varies widely, and both zoning pattern and core/rim structure are indeterminable for many of these grains. Mineral inclusions ≥1 μm were analyzed by energy-dispersive spectrometry and identified by comparing the inclusion X-ray energy spectra with spectra from standard materials.

X-ray fluorescence (XRF) analyses of 17 major, minor, and trace elements were made from whole-rock samples by XRAL Inc. Both fused disc and pressed powder analyses were calibrated against standard reference materials BCS267 and XRAL04.

4.3. Ion microprobe (SHRIMP II) U–Th–Pb isotopic analysis

Zircons in Au-coated mounts were analyzed during the course of 10 analytical sessions totaling ∼200 h over a ten month period. The majority of the analytical work was undertaken on SHRIMP II at the Chinese Academy of Geological Sciences in Beijing, with a few additional analyses performed using the SHRIMP II at Curtin University (run 5). In situ U–Th–Pb age determinations on ∼25 μm diameter spots in individual grains were made following standard operating procedures (Nelson, 1997; Williams, 1998). A complete analysis consisted of seven cycles of measurements at each mass ($^{196}(Zr_2O)$, ^{204}Pb, $^{204.045}Pb_{(bkg)}$, ^{206}Pb, ^{207}Pb, ^{208}Pb, ^{238}U, $^{248}(ThO)$, and $^{254}(UO)$). To increase the overall number of grains surveyed, all of the zircons were first analyzed in ‘reconnaissance’ mode, where only one cycle of measurements lasting ∼3 min was made. The precision of single-cycle analyses was lower by up to a factor of 5, however, accuracy was typically within 10–50 Ma of the subsequent seven-cycle analysis on the same spot. One-cycle analyses thus provide a rapid determination of the uncorrected $^{207}Pb/^{206}Pb$ ratio, which is a reliable method for quickly identifying ‘old’ grains. When the uncorrected $^{207}Pb/^{206}Pb$ ratio indicated an age in excess of 3800 Ma, a full seven-cycle analysis was performed (Table 2). Zircon U/Pb concentration standards used were CZ3 ($^{238}U/^{206}Pb$ age = 564 Ma: Pidgeon et al., 1994) and TEMORA 1 ($^{238}U/^{206}Pb$ age = 417 Ma: Black et al., 2003). Standard results for the 10 analytical runs in the form (*x*, *y*, *z*), where *x* is the run number, *y* the number of analyses, and *z* the Pb/U calibration error in 1σ% are reported as follows: CZ3 [(1, 25, 0.79), (2, 21, 0.98), (5, 13, 1.23), (8, 15, 1.84), (9, 30, 0.99), (10, 12, 2.53)] and TEMORA 1 [(3, 4, 0.81), (4, 5, 3.04), (6, 21, 1.09), (7, 3, 0.89)]. All raw SHRIMP data files were reduced with Squid (Ludwig, 2001b), and histograms were plotted using Isoplot/Ex (Ludwig, 2001a).

5. Results

5.1. Approach to U/Pb concordance, Th–U chemistry, age determination

A total of 140 seven-cycle analyses were made on grains where an age ≥3800 Ma was indicated by the one-cycle analysis, or on selected younger grains (Table 2).

Using a combination of CL and BSE imaging, and the U/Pb age, analysis locations were classified as occurring in either a core or rim domain (Table 2). Most grains that were analyzed in multiple spots yield concordant analyses that are homogeneous in age or zoned with younger rims. However, several grains yield both concordant and highly discordant analyses from the same CL domain, and a range of ages that are not geologically reasonable for a single stage of growth. For grains with multiple analyses, the oldest age is typically the most concordant. Most discordant analyses are located on visible cracks, and yield younger $^{207}Pb/^{206}Pb$ ages relative to analyses on nearby concordant, crack-free spots. Interestingly, several highly discordant analyses located on cracks yield $^{207}Pb/^{206}Pb$ ages that approximate our preferred age based on a concordant analysis in the same grain (see discussion below). Hence, analyses located on

cracks do not always result in disturbed $^{207}Pb/^{206}Pb$ ratios.

Recent Pb-loss has been demonstrated to be the major cause of discordance in the Jack Hills zircons based on multiple single-grain analyses (Wilde et al., 2001), however, ancient Pb-loss within individual grains prior to deposition of the Jack Hills sediments cannot be disproved. Values of U–Pb concordance (Table 2) for individual analyses range from 103 to 7%. Fig. 3 shows elemental U and Th abundances and Th/U ratios plotted against percentage of U–Pb concordance for all analyses in Table 2 (three <20% concordant analyses with exceptionally high U and Th values are not plotted). The data show non-linear increases in the average U, Th, and Th/U ratio as the analyses become less concordant. Above 75% concordance, the average U abundance is higher than the average Th, whereas at 75% concordance, a cross-over occurs, below which the average Th is higher than the average U abundance. While analyses less than 75% concordant may simply be a consequence of analyzing radiation damaged areas, actinide-rich grains, or inclusions, the cause of the increased Th/U ratio is less clear, as both U loss and Th enrichment will result in an increased Th/U ratio. Whatever the cause, below 75% concordance the analyzed areas are enriched in Th over U, resulting in higher average Th/U ratios.

The interpretation of disparate ages from a single grain is a problem for all ion microprobe studies of U–Pb ages in Archean zircons. We have addressed this by adopting the convention whereby only analyses ≥85% concordant are considered to preserve primary age information based on the following considerations. The significantly higher values of Th abundance and Th/U ratio for samples below 80% concordance accompanies higher Pb-mobility (as inferred by concordance), and signifies a higher degree of isotopic disturbance or elemental mobility in these analysis areas relative to spots that yielded more concordant analyses (Fig. 3). The Th–U data can thus be used as an additional proxy for Pb-mobility when evaluating age determinations. In addition to only considering ≥85% concordant analyses, where multiple analyses of a grain were made, the oldest (and usually the most concordant) $^{207}Pb/^{206}Pb$ analysis is interpreted as its crystallization age. The procedure of interpreting the oldest

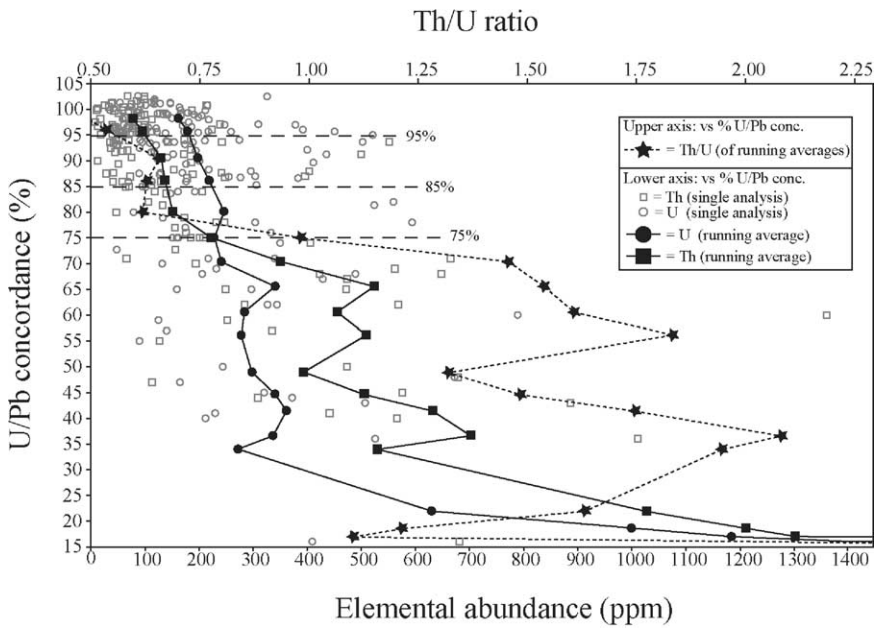

Fig. 3. Elemental Th and U abundances (lower *x*-axis) and Th/U ratio (upper *x*-axis) plotted against percentage of U–Pb concordance for the 140 seven-cycle analyses in Table 2. Averages of Th, U, and Th/U ratio were calculated as 10% running averages at 5% increments of concordance beginning with 100%. Each running average includes all data points in a bin that extends over ±5% concordance from the given increment (i.e. a running average calculated at 90% concordance averages all data points that are 85–95% concordant).

$^{207}Pb/^{206}Pb$ age in an individual >4000 Ma zircon as the minimum age of crystallization and younger ages as artifacts of ancient Pb-loss has been described previously (Compston and Pidgeon, 1986; Wilde et al., 2001; Nelson, 2002), and assumes that Pb-mobility is non-uniform within a given crystal. The incorporation of unsupported ^{231}Pa during zircon crystallization has been proposed for producing artificially elevated $^{207}Pb/^{206}Pb$ ages within zircons (Parrish and Noble, 2003), however this speculative process is difficult to document and has not be proven in any suite of zircons. For zircons from this study, we favor Pb-loss to explain variable ages within individual zircons, and have listed the preferred $^{207}Pb/^{206}Pb$ crystallization ages as bold font in Table 2.

5.2. Early Archean zircons (4350–3800 Ma)

Forty-one grains were identified that yielded ages ranging from 4348 to 3904 Ma; all except three occur in West Transect samples (Table 2). The 41 grains fall into the following age ranges: 4350–4250 ($n = 4$), 4200–4000 ($n = 32$), and 4000–3800 Ma ($n = 5$) (Fig. 4). No grains were found in the intervals 4250–4200 and 3900–3800 Ma. Elemental Th and U compositions of the 41 'preferred age' analyses on these grains (one analysis per grain) range from 8 to 404 (average = 81), and 35–451 ppm (average = 160), respectively, and the Th/U ratio ranges from 0.04 to 1.41 (average = 0.52). Grains older than 4300 Ma include 4324 ± 6 (Fig. 5b), 4324 ± 18 (Fig. 5e), and 4348 ± 3 Ma (Fig. 5h). The most common pattern observed in the CL images is oscillatory zoning (Fig. 5). Oscillatory growth zoning is preserved in nearly all imaged grains (with the exception of Fig. 5e, t, and x). Sector zoning is present in eight grains (Fig. 5a, f, j–l, n, p, and r) and patchy zoning in portions of five grains (Fig. 5e, o, q, t, and x). Other CL textures are also discernable. Grain 54-77 (Fig. 5b) contains an oscillatory zoned core with embayed margins that appears to be half of a melted and/or broken inherited zircon. Grain 54-34 (Fig. 5c, see arrows) has a structureless curvilinear zone along its margin that surrounds an oscillatory zoned core. The irregular margin is likely to have resulted from solid-state recrystallization along the grain boundary (Pidgeon, 1992). Grain 54-37 (Fig. 5p) displays mosaic-like sector zoning, with faint concentric zoning preserved in some areas. This sector zoning is similar to zoning observed in recrystallized zircons from granulite-facies sediments (Vavra et al., 1996). With few exceptions, the majority of the other zircons preserve simple zoning patterns that record their growth in magmas.

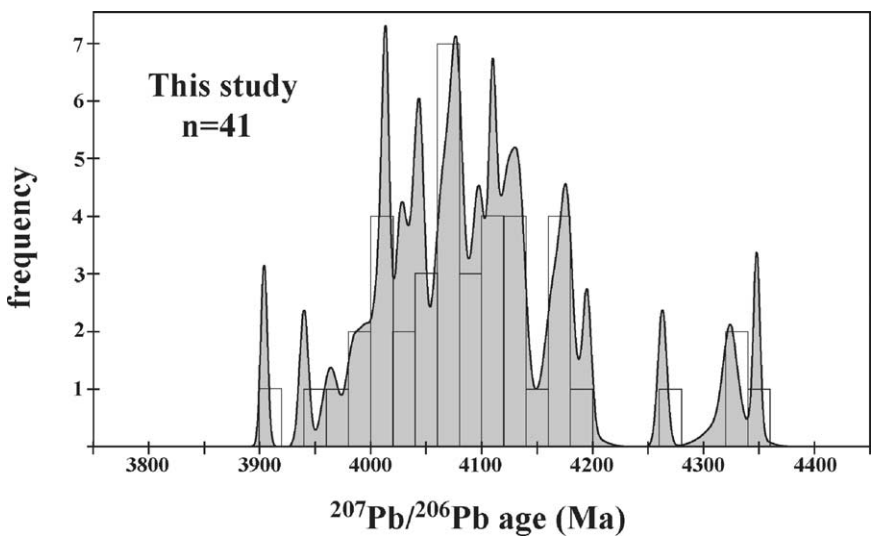

Fig. 4. Combined histogram and Gaussian summation probability density plot of 41 ≥3800 Ma detrital zircons from Jack Hills with seven-cycle ion microprobe analyses from this study. Only one age per grain is plotted (criteria discussed in text); bin width = 20 Ma.

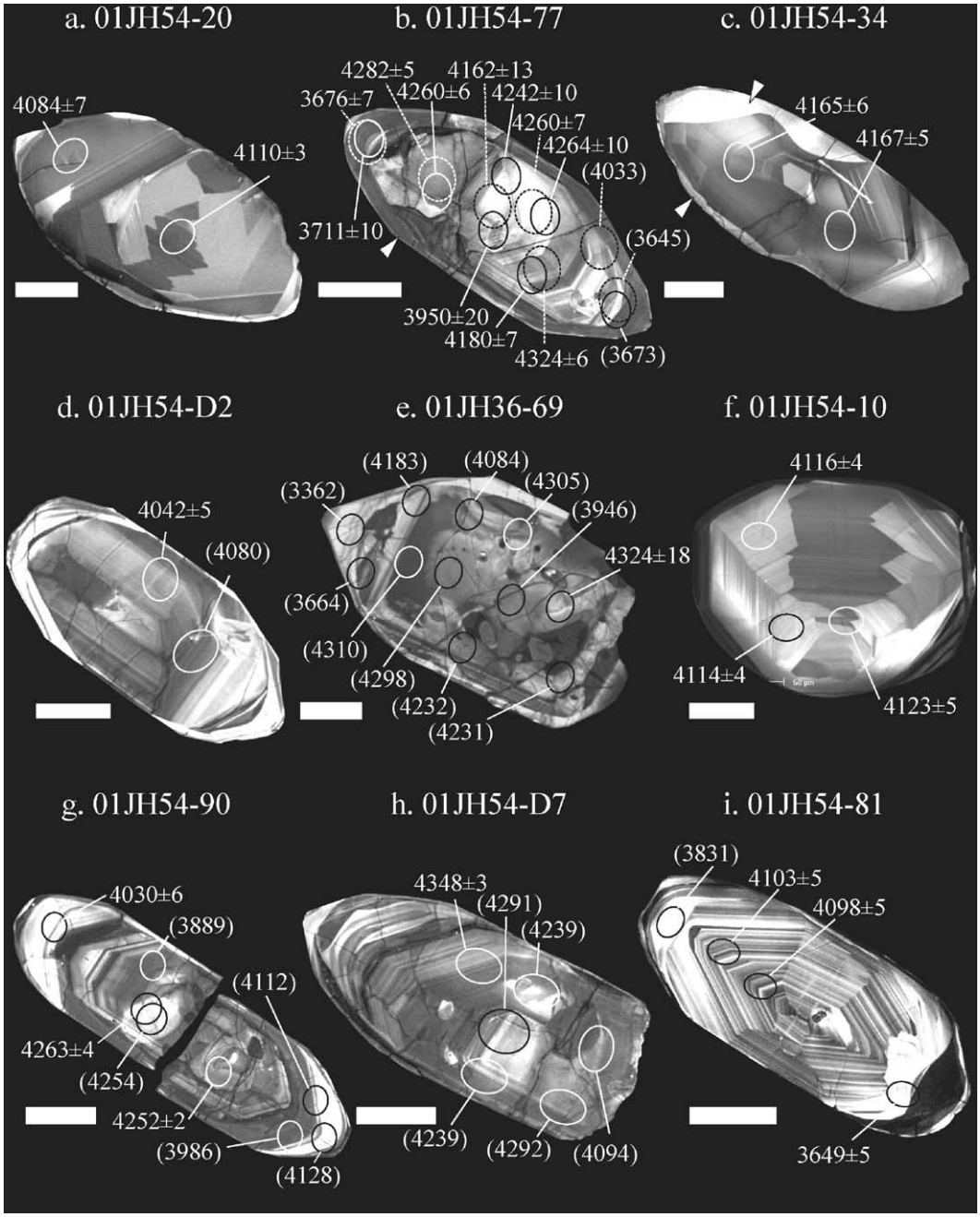

Fig. 5. CL images of selected zircons. Circles show location of SHRIMP II analyses. Precise ages given in Ma with 1σ errors. Ages <85% concordant are listed in parentheses with the error omitted. The bright ovals in (g), (w), and (x) are the areas rastered prior to analysis. White arrows point to features mentioned in text; scale bars are all 50 μm.

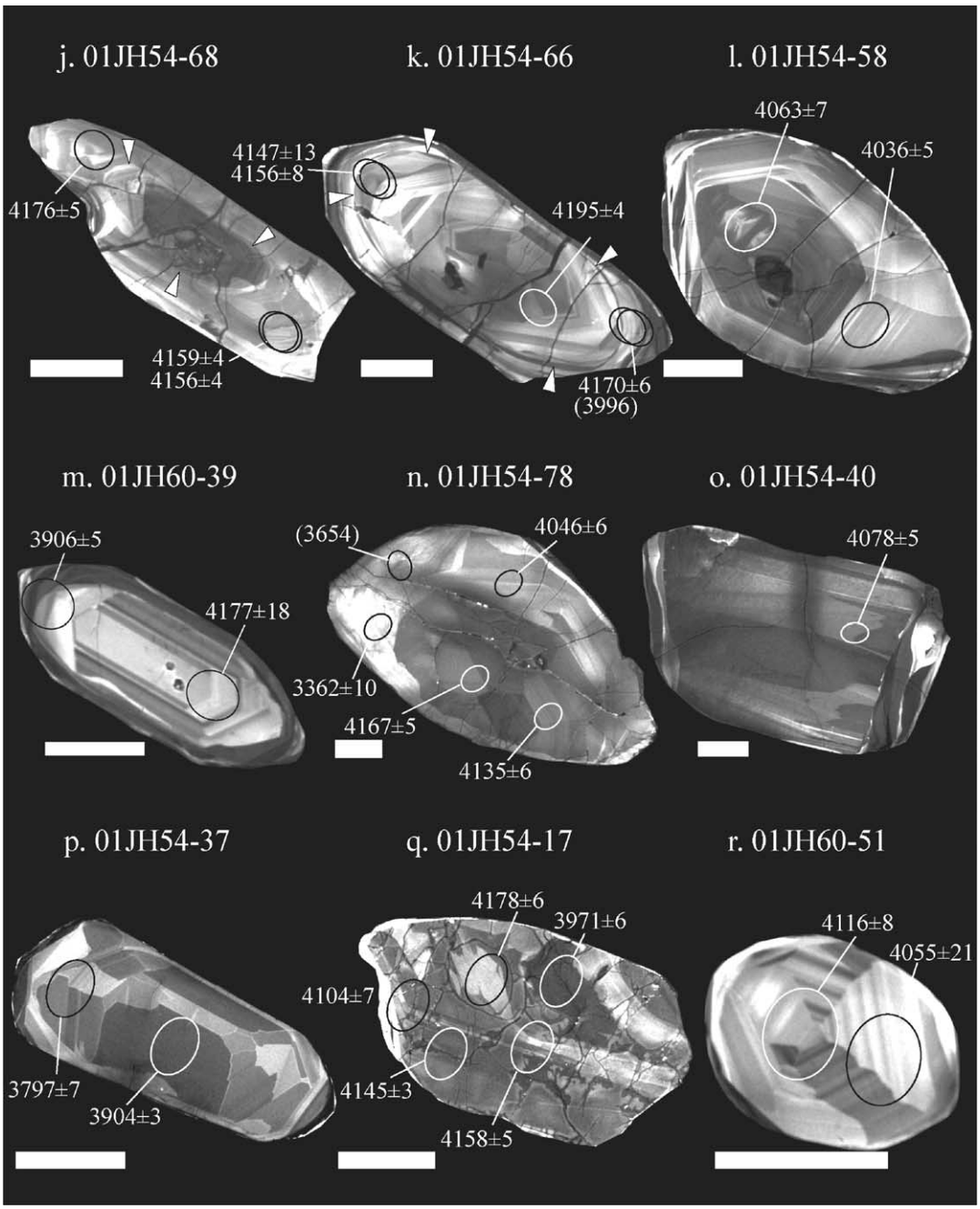

Fig. 5. (*Continued*).

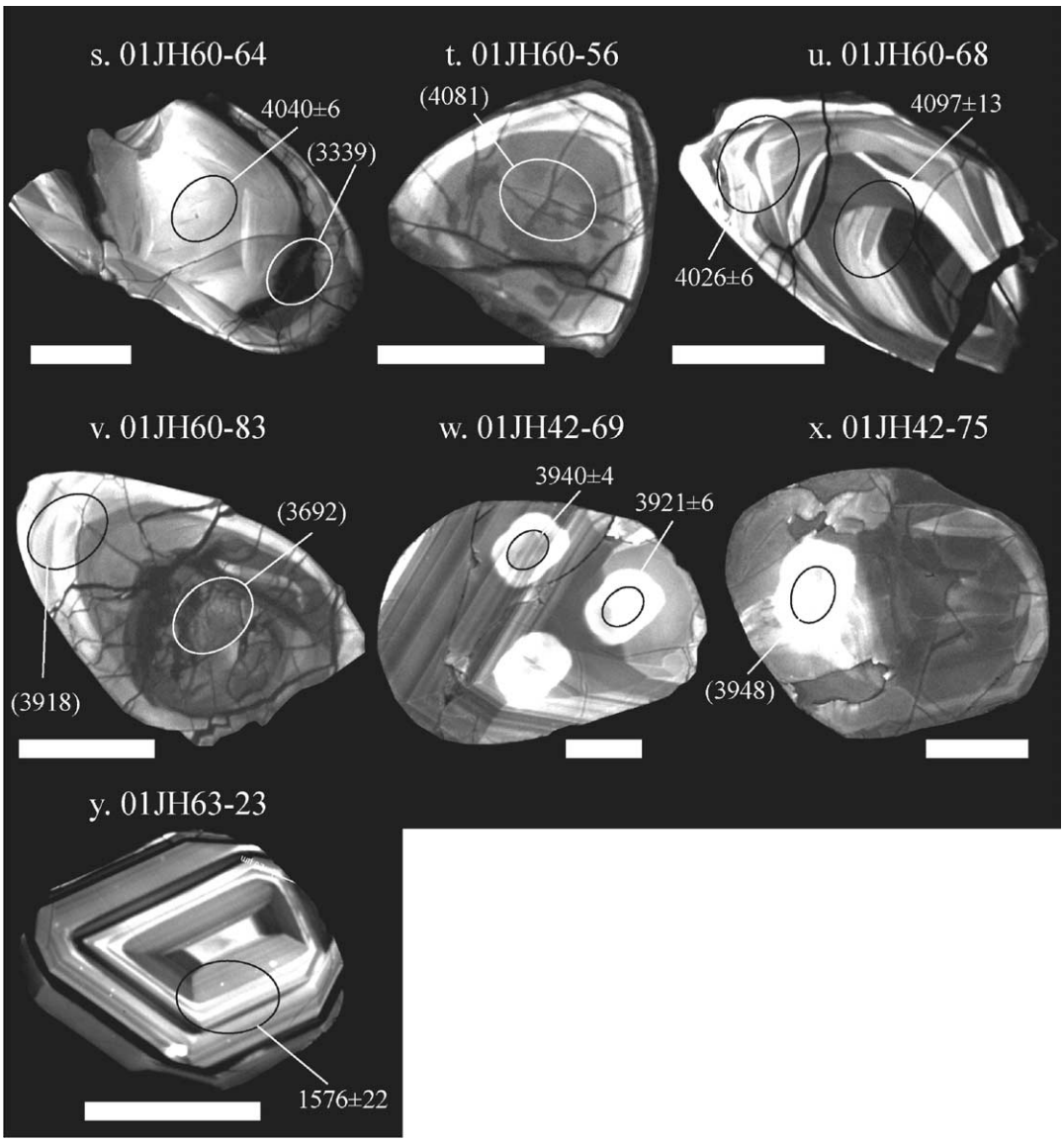

Fig. 5. (*Continued*).

Younger rims were identified on many of the >3800 Ma grains (Fig. 5b, e, g, i–k, m, and n). Most overgrowths truncate zoning in the core, and yield brighter (Fig. 5d, e, g, n) or darker (Fig. 5b, i, m) CL intensities than the core area they surround. Establishing the ages of the overgrowths proved difficult, as many of the analyses are highly discordant (located on cracks) or appear to overlap the sometimes thin rim into the core area resulting in a mixed age. Grain 54-77 (Fig. 5b) is surrounded by a euhedral overgrowth with fine oscillatory zoning (see arrow). The overgrowth yields concordant ages of 3676 ± 7 and 3711 ± 10 Ma from one grain termination, and highly discordant ages of 3645 ± 7 and 3673 ± 10 Ma from the other. Despite their similarity in age, all four of these analyses include a component of the inherited core (Fig. 5b), and thus the apparent ca. 3690 Ma age may be a mixed age. The Th/U ratios of the two concordant overgrowth analyses

(Th/U = 0.25) are lower than the range found in the core (Th/U = 0.45–1.43), but are still in the range of igneous Th/U values. Grain 36-69 (Fig. 5e) contains a distinctive euhedral overgrowth, however, the only analysis that does not overlap with the core area yields a highly discordant age of 3362 ± 20 Ma, which is noteworthy but may not be the primary age. Grain 54-90 (Fig. 5g) yields a core age of 4263 ± 4 Ma, and attempts at analyzing the euhedral overgrowth yielded mixed or discordant ages (located on cracks). A less discordant age of 4030 ± 6 Ma in a bright CL area is the best estimate for the age of the overgrowth. Grain 54-81 (Fig. 5i) yields a core age of 4100 ± 4 Ma (weighted mean of two concordant analyses), and also contains a dark, rounded rim. Due to cracks, no analysis was made in the overgrowth area, but an analysis of the core/rim boundary where the zoning is clearly disturbed yields an age of 3649 ± 5 Ma. Grain 54-81 is one of the only grains where the Th/U ratio of the overgrowth (0.06) is much lower than values in the core (0.43), which suggests a metamorphic origin for the rim. Grains 54-66 and 54-68 (Fig. 5k and j, respectively) preserve oscillatory zoned xenocrystic cores outlined by smooth dissolution surfaces (see arrows), and contain oscillatory zoned overgrowths. Grain 54-66 contains a large rounded core with an age of 4195 ± 4 Ma. Four attempts to date the overgrowth yielded mostly mixed ages, resulting in only one concordant age clearly outside the core at 4170 ± 6 Ma. Grain 54-68 (Fig. 5j) contains an overgrowth that yields an age of 4176 ± 5 Ma on one termination, and two spots with a weighted mean of 4158 ± 3 Ma from the opposite end. Unfortunately, no age was determined on the inherited core due to the presence of excessive cracks. Grain 60-39 (Fig. 5m) yields a core age of 4177 ± 18 Ma and contains a euhedral overgrowth with an age of 3906 ± 5 Ma, however a small portion of the core area may have been included in the overgrowth spot. Grain 54-78 (Fig. 5n) yields near concordant core ages of 4167 ± 5 and 4135 ± 6 Ma in the inner core, and an age of 4046 ± 6 Ma in the outer core. Of two attempts to date the rim, one yielded a near concordant age of 3362 ± 10 Ma. The Th/U ratio of the concordant rim (Th/U = 0.41) is indistinguishable from the range observed in three core analyses (Th/U = 0.39–0.45).

Physical characteristics of the 41 ≥3800 Ma grains from this study (and two additional grains reported by Peck et al., 2001), including size, aspect ratio, color, shape, and mineral inclusions, are listed in Table 3. The sizes of the zircons vary, ranging from 60 to 425 μm in maximum dimension. Aspect ratios are generally low, ranging from 1:1 to 1:3.4 (average = 1:1.7), and in some cases have been modified by varying degrees of rounding during sedimentary transport and/or breakage during separation (e.g. Fig. 5s, w, x). Grain color and clarity (when viewed cast in epoxy and polished, in transmitted light) varies from light pink and transparent to dark red. Grain morphologies include a spectrum from euhedral to well rounded, with one and sometimes two pyramids preserved on many of the zircons. While generally inclusion-poor, silicate and phosphate inclusions larger than 1 μm were identified in several grains by energy-dispersive spectrometry, and include quartz, muscovite, apatite, monazite, and xenotime.

5.3. Younger Archean zircons (3800–2500 Ma)

Identifying zircons younger than 3800 Ma was not the emphasis of this study, and as such they are not described in as much detail. The limited number of seven-cycle analyses on <3800 Ma zircons listed in Table 2 is therefore not a representative sampling. Middle Archean zircons (here used as 3800–3300 Ma) were only analyzed in one Jack Hills sample. Quartzite 01JH36 contains two concordant zircons with cores 3652 ± 7 (36-5) and 3681 ± 3 Ma (36-86) old, and one less concordant grain at 3561 ± 47 Ma (36-140). While only three grains, these zircons demonstrate that Meeberrie gneiss age zircons (3730–3600 Ma) occur within the Jack Hills sediments (Compston and Pidgeon, 1986; Nutman et al., 1991). Late Archean zircons (here used as 3300–2500 Ma) were found in samples from both transects. In the East transect 01JH47 contains two late Archean zircons that yield ages of 2724 ± 7 (47-b-2) and 2504 ± 6 Ma (47-b-3). Sample 01JH63 also contains nearly concordant late Archean zircons with similar ages to those found in 01JH47, including 2736 ± 6 (63-1), 2620 ± 10 (63-27), and 2590 ± 30 Ma (63-36).

5.4. Proterozoic zircons (2000–1600 Ma)

One of the more surprising results is the discovery of a suite of Proterozoic zircons from sample 01JH63 in the West Transect. Three nearly concordant zircons were identified with Proterozoic ages of 1973 ± 11

Table 3
Properties of 43 >3800 Ma Jack Hills zircons ≥85% concordant in U–Pb age

Sample grain	Size (μm)	Aspect ratio (1:*x*)	Color-clarity[a]	Shape	CL zoning	Inclusions >1 μm
01JH36-69	320 × 200	1.6	3-o	f, 1P	p	Xenotime, quartz
01JH36-115	175 × 125	1.4	2-c	f	o	–
01JH42-69	220 × 155	1.4	2-c	r	o	–
01JH54-10	225 × 175	1.3	1-c	s, r	o, s	–
01JH54-17	400 × 210	1.9	3-o	e, 1P	o, p	Quartz
01JH54-20	300 × 160	1.9	3-c	e, r, 2P	o, s	–
01JH54-34	350 × 140	2.5	3-c	e, r, 2P	o	–
01JH54-37	375 × 150	2.5	3-c	e, r, 2P	o	–
01JH54-40	350 × 200	1.8	2-c	r, 2P	o, s, p	–
01JH54-58	275 × 170	1.6	2-c	r, 2P	o, s	Quartz
01JH54-66	325 × 125	2.6	1-c	e, r, 2P	o, s	Muscovite/quartz/Fe-oxide
01JH54-68	290 × 105	2.8	1-c	e, r, 2P	o	–
01JH54-77	280 × 110	2.5	1-c	e, r, 2P	o	–
01JH54-78	405 × 240	1.7	3-o	r	o	–
01JH54-81	280 × 120	2.3	1-c	e, r, 2P	o	Apatite (x2)
01JH54-90	425 × 125	3.4	1-o	e, r, 2P	o	–
01JH54-D2	230 × 105	2.2	1-c	e, r, 2P	o	–
01JH54-D7	240 × 105	2.3	1-c	r, 1P	o	Xenotime, quartz
01JH60-39	200 × 60	3.3	1-c	e, r, 2P	o	–
01JH60-51	120 × 80	1.5	1-c	s, r, 2P	o	–
01JH60-64	140 × 105	1.3	1-c	r, 1P	o	Apatite (x3)
01JH60-68	155 × 90	1.7	1-c	e, r, 2P	o	–
01JH65-22[b]	60 × 50	1.2	n.a.	f	n.a.	–
W74/2-36[c]	260 × 220	1.2	2-o	f	o	Quartz
W74/2-52[c]	245 × 180	1.4	n.a.	f, 1P	o	–
W74/3-7	190 × 110	1.7	1-c	f	o	–
W74/3-13	90 × 70	1.3	2-c	f	p	–
W74/3-15	150 × 90	1.7	2-c	r	o	–
W74/3-30	160 × 125	1.3	3-c	r	p	–
W74/3-36	200 × 90	2.2	2-c	f	o	–
W74/3-41	125 × 100	1.3	1-c	f	o	–
W74/3-58	175 × 120	1.5	2-c	f	o	–
W74/3-62	150 × 140	1.1	2-o	r	p	–
W74/3-114	140 × 100	1.4	3-c	f	o, s	–
W74/3-127[b]	200 × 140	1.4	1-c	e, r, 2P	n.a.	–
W74/3-131	210 × 125	1.7	3-o	f	p	–
W74/3-133	180 × 140	1.3	2-c	f	o	–
W74/3-134	200 × 125	1.6	1-c	e, 1P	o	–
W74/3-143	125 × 100	1.3	3-o	e	p	–
W74/3-152	140 × 60	2.3	3-c	f	o	–
W74/3-154	120 × 100	1.2	1-c	r	p	–
W74/3-170	120 × 80	1.5	1-c	f	o	–
W74/3-174	170 × 170	1.0	2-c	f	o, s	–

Shape — s: stubby, r: rounded, e: elongate, f: fragment, *x*P: number of pyramids preserved. CL zoning — o: oscillatory, s: sector, p: patchy; n.a.: not analyzed.

[a] Color and clarity of mounted grain as viewed through the polished surface in transmitted light — 1: colorless to light pink, 2: pink to red, 3: dark red, brown, c: clear, o: opaque.

[b] Grain lost during subsequent processing.

[c] Age, CL image, and inclusion data previously published in Peck et al. (2001).

(63-7), 1752 ± 22 (63-53), and 1576 ± 22 Ma (63-23) (Table 2). While the CL images of the two older grains are ambiguous, grain 63-23 preserves undisturbed oscillatory zoning, indicative of igneous zircon (Fig. 5y). These are the youngest detrital zircons reported from Jack Hills (Cavosie et al., 2002b). Such unusual ages might raise concerns that sample contamination occurred, however, Dunn et al. (2002) reported similar Proterozoic ages in Jack Hills from rocks in the same area. As hand-samples with cross-cutting veins were avoided for zircon separation, these Proterozoic age zircons appear to be of detrital origin and are discussed further below.

5.5. Zircon age distributions in Jack Hills metasediments

Eleven-hundred one-cycle ion microprobe analyses of the $^{207}Pb/^{206}Pb$ ratio were made on zircons from 10 samples. Histograms of the results correlated to stratigraphy are plotted in Fig. 6, with the number in parentheses indicating the number of grains plotted (see caption, Fig. 6). The largest component of all detrital populations consists of 3500–3250 Ma zircons, which correlate with the ages of the Eurada and Dugel gneisses (Kinny and Nutman, 1996). A second population found in all samples, 3750–3500 Ma zircons, can only be correlated to the Meeberrie gneiss, as these ages do not overlap with ages found in other gneisses in the Narryer Terrane. The 3250–3000 Ma zircons occur in all samples, except 01JH113 and 01JH65, and are most prominent in the East Transect. Zircons of similar age have been found as minor components in the Dugel and Eurada gneisses (Kinny et al., 1990; Nutman et al., 1991).

Zircons younger than 3000 Ma were found as a minor component in East Transect samples, and also in one West Transect sample, 01JH63. In the East transect, 2750–2500 Ma zircons form a small population and may correlate to the ca. 2650 Ma granitoids described by Pidgeon and Wilde (1998). The age distribution in quartzite sample 01JH63 is markedly different from any other sample from the Jack Hills. Along with the previously mentioned populations from 3750 to 3000 Ma, it includes peaks from 3000 to 2500 Ma and several younger grains in the interval 2000–1600 Ma. As in the East Transect, the 2750–2500 Ma peak may be correlated with the ca. 2650 Ma granitoids described by Pidgeon and Wilde (1998). The Proterozoic zircons do not correlate with any known rocks in the Narryer Terrane.

Zircons older than 3800 Ma were found as a small component in nearly all samples, with the notable exception of 01JH63 and 01JH113. All of the >3800 Ma zircons are from an unknown source, as no ca. 3800 Ma rocks have been identified in Western Australia. However, zircons older than 4000 Ma were restricted to the four northernmost samples from the West Transect and quartzite sample 01JH36, located between the transects. Thus, it appears all known >4000 Ma zircons in the Jack Hills are located within 1 km from the original W74 locality.

6. Discussion

6.1. Early Archean magmatism

If the majority of the ≥3800 Ma zircons from this study are igneous, as indicated by the CL images, then they must have originated during early Archean rock-forming events. A histogram of ≥3800 Ma detrital zircon ages from Western Australia, including the results from this study and others, is shown in Fig. 7, where each datum represents the oldest concordant analysis of a given grain. There are concentrations of ages in the intervals from ca. 4400 to 4250, 4200 to 4000, and several peaks from 4000 to 3800 Ma, which allow magmatic events older than the rock record to be resolved. The earliest magmatic interval, from 4400 to 4250 Ma, is prolonged, however resolution of sub-intervals is less certain as only a limited number of grains have been identified older than ca. 4250 Ma. The period from 4200 to 4000 Ma contains the majority of the zircons, and appears to be a major period of continuous igneous activity, lasting roughly 200 Ma. Within this interval, several sub-intervals are resolvable. Smaller peaks at 3920–3900 and 3840 Ma may also represent discrete igneous events. The age distribution also contains conspicuous gaps (Fig. 7). No record of activity in the intervals from 4250 to 4200 and 3900 to 3850 Ma has been found. These gaps may represent periods of magmatic quiescence, or alternatively may result from selective preservation/sampling. The fact that there are discrete ‘peaks’ and ‘gaps’ within this distribution is further evidence that the U–Pb systems of the zircons have not

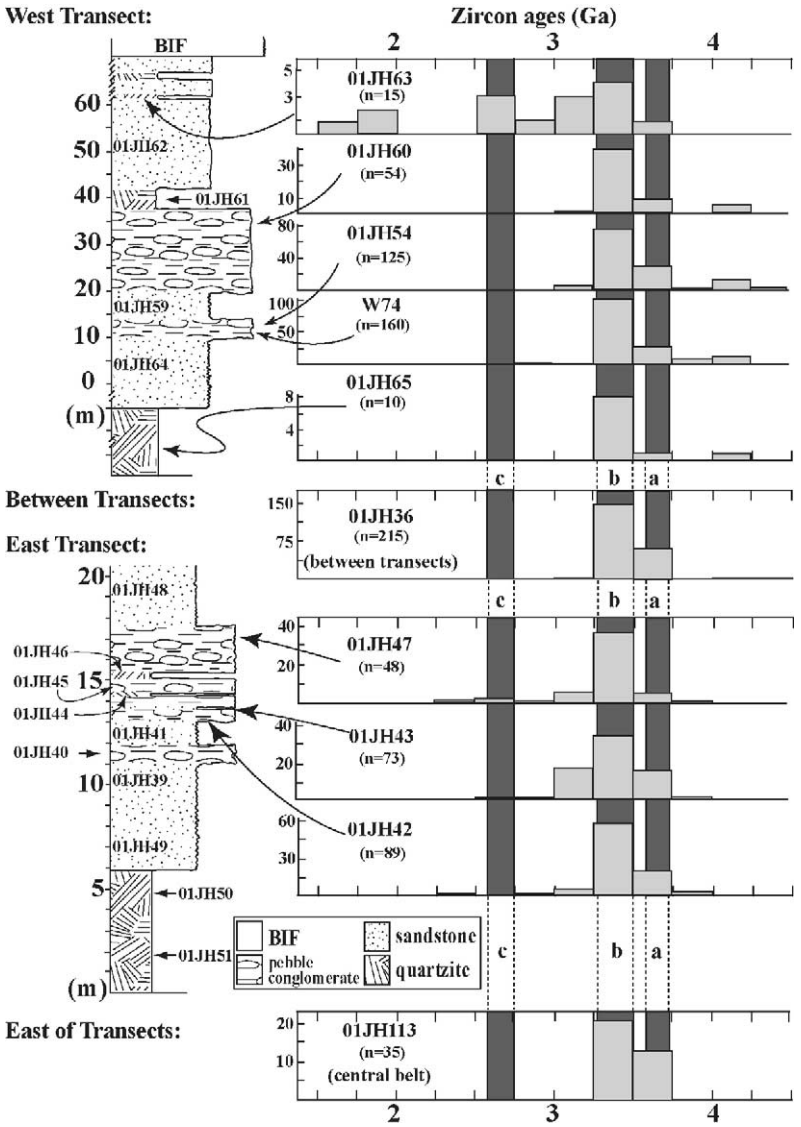

Fig. 6. Stratigraphic columns of the West and East transect sample locations with histograms of $^{207}Pb/^{206}Pb$ ages for detrital zircons. The histograms were constructed from the results of the one-cycle analyses, and pool all analyses where the cps on ^{204}Pb for the one-cycle were less than 50 (probably the result of contamination from the Au coat). Analyses with more than 50 counts on ^{204}Pb were rejected. Background counts on ^{204}Pb were typically 0–5 cps, resulting in a signal-to-background ratio that was usually below 10:1. Applying the above criteria allowed 824 of the 1100 one-cycle analyses (75%) to be used (Appendix B). The value in parentheses beneath the sample number is how many analyses are included in each histogram. Bin width is 250 Ma. These histograms are quantitative but the ages have a larger uncertainty than the seven-cycle analyses. They provide a general picture of the detrital age populations. Note changes in the frequency scale between histograms. Shaded vertical stripes indicate known igneous events in the Narryer Terrane: (a) 3730–3600 Ma component of Meeberrie gneiss, (b) Eurada (3490–3440 Ma) and Dugel gneisses (3380–3350 Ma), and (c) 2750–2600 Ma granitoids. Granitoid references listed in the text.

been completely reset by younger thermal events, as this would tend to 'smooth' the distribution. While the statistics of this sample set will improve as more analyses are reported, it is worthy of note that the magmatic intervals identified in Fig. 7 are clearly evident in the smaller sample shown in Fig. 4.

The causes of the early rock-forming events are unknown, however, various aspects of the zircons allow constraints to be placed on their petrogenesis. Any proposed igneous environment must be capable of producing the characteristics of the zircons described in this study, particularly their internal zoning and euhedral morphology. In addition, the presence of SiO_2 inclusions within ca. 4400–4000 Ma zircons (Maas et al., 1992; Wilde et al., 2001; Peck et al., 2001; this study) requires that felsic differentiation occurred, though the volumes of felsic rock formed are difficult to evaluate. Other lines of evidence, such as elevated $\delta^{18}O$ values (Wilde et al., 2001; Mojzsis et al., 2001; Peck et al., 2001), mineral inclusions, and trace elements including REE (Maas et al., 1992; Wilde et al., 2001; Peck et al., 2001) have also been used to infer granitic compositions (sensu latu) for the parent rocks of the >4000 Ma zircons. One additional line of evidence from this study that suggests the source rocks were felsic is the presence of xenocrystic cores within two grains (Fig. 5j and k) that have 4175–4150 Ma rims. While only two grains, the survival of these cores indicates that some grains were recycled into zircon-saturated magmas and ca. 4150 Ma that were felsic in composition (Watson and Harrison, 1983; Maas et al., 1992; Peck et al., 2001; Miller et al., 2003).

There are many well-documented processes and/or environments that may have generated the suspected felsic parent rocks of the zircons in this study, including tectonics along convergent or divergent margins and large-scale volcanism in plume-dominated regimes. Felsic rocks are common along convergent margins, including subduction zone environments, and also along divergent margins, as exemplified by the rhyolites at Icelandic volcanic centers (Gunnarsson et al., 1998). Large-scale volcanism can also create felsic rocks, calderas, and the re-melting of crust in the absence of either convergent or divergent tectonics (Bindeman and Valley, 2001). In the Early Archean, large continents did not exist and volcanism may have been dominated by plumes. Geologic literature abounds with descriptions of zircons with similar features to those here described in Jack Hills zircons. Whether or not magmatic processes similar to those described above were operative during the Early Archean is unknown, however, the abundance of >3800 Ma

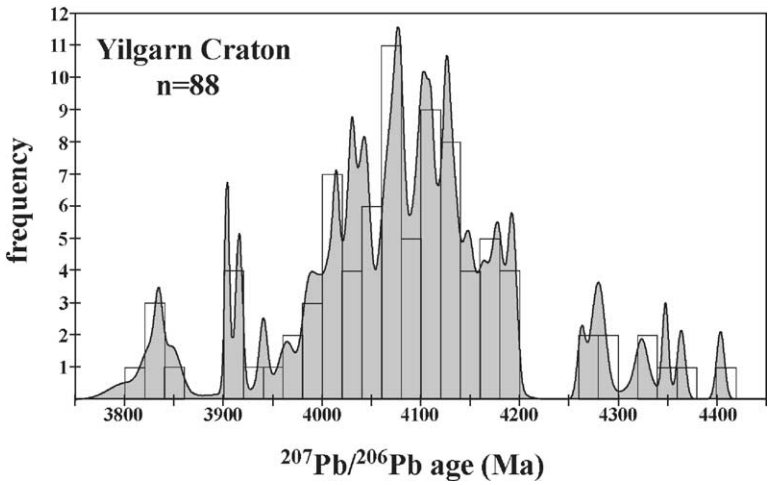

Fig. 7. Histogram and Gaussian summation probability density plot of 88 ≥3800 Ma detrital zircons with seven-cycle U/Pb ion microprobe ages from the Yilgarn Craton, Western Australia. Same grain selection criteria as Fig. 4 (i.e. only one age, ≥85% concordant per crystal). Data sources are as follows. Jack Hills: This study ($n = 41$), Compston and Pidgeon (1986) ($n = 17$), Wilde et al. (2001) ($n = 1$), Peck et al. (2001) ($n = 3$), Mojzsis et al. (2001) ($n = 4$), Maas et al. (1992) ($n = 10$); Nelson (2000) ($n = 2$); Mt. Narryer: Froude et al. (1983) ($n = 4$), Nutman et al. (1991) ($n = 4$); Barlee Terrane: Wyche et al. (2004) ($n = 3$); bin width = 20 Ma.

zircons in the Jack Hills sediments and the variable age sources indicate that prolonged, large-scale magmatic processes occurred, and culminated in the formation of a granitic (sensu latu) protocrust prior to 4000 Ma.

6.2. Are the Jack Hills zircons the result of impacts?

It is also possible that some of the Jack Hills zircons grew in melts related to large meteorite impacts. On the early Earth, a single large impact could have melted an entire hemisphere (Melosh, 1989), although no evidence for large terrestrial impacts or widespread impact-induced magmatism during the Early Archean has been found thus far. However, lunar craters, such as Orientale (>900 km diameter), are evidence that large impacts were occurring near and probably on Earth as late as 3800 Ma (French, 1998). In addition, the largest recognized terrestrial impact structures, the Sudbury (Canada) and Vredefort (S. Africa), are 200–300 km in diameter and both formed ca. 2000 Ma, supporting the idea that still larger impacts occurred on the young Earth when the Jack Hills zircons were being formed (French, 1998).

Zircons reported in target rocks affected by shock waves from impacts have been shown to preserve shock-related microstructures (Bohor et al., 1993), however, these features have not been reported in Jack Hills zircons. In the absence of shocked zircons, the critical question is if euhedral oscillatory zoned zircons can form within magmas generated by impacts. While impact-induced melt rocks are known, melt rocks in most terrestrial craters are limited in extent (where present), and contain quench textures indicative of relatively short cooling histories (French, 1998) that make this environment an unlikely place for forming the Jack Hills zircons. A study of granophyres and breccias from the Vredefort impact found that zircons from the melt sheet are typically small, usually 50–150 μm long, and euhedral, transparent, gem-quality zircons (Kamo et al., 1996). Zoning in these grains was not reported. A study of zircons from lunar granophyres noted that oscillatory zoning is rare, and that grains are typically small (30–100 μm long) and not euhedral (Meyer et al., 1996). In terms of size and internal zoning, Jack Hills zircons bear little resemblance to zircons from the granophyres described above, and thus far do not appear to have an impact origin.

6.3. Evidence for >4000 Ma crust in the evolution of the Yilgarn Craton

Rim ages from 3690 to 3362 Ma on >4000 Ma grains are a direct record that the earlier formed crust survived long enough to participate in younger tectonic events in the Narryer Terrane. These rim ages overlap with ages reported for granitoids in the vicinity of Jack Hills (Kinny et al., 1988; Kinny and Nutman, 1996; Pidgeon and Wilde, 1998). The two older rims at ca. 3690 (Fig. 5b) and 3650 Ma (Fig. 5i) overlap with zircon ages from the Meeberrie gneiss (Kinny and Nutman, 1996). The 3362 ± 10 Ma rim (Fig. 5n) may have formed during the intrusion of the Dugel gneiss precursors. These three grains differ in rim morphology and age, but are likely to have been recycled from their original igneous hosts into the precursors of the gneisses between ca. 3700 and 3400 Ma ago. Subsequently, overgrowths formed on the zircons, they were eroded, and eventually deposited in the Jack Hills sediments.

The preservation of recycled material in both the Meeberrie and Dugel gneisses has previously been discussed (Section 2.1), however, no >4000 Ma zircon ages have been recorded in enclaves (Kinny et al., 1988) or in samples of the gneisses. The correlation of the ca. 3690 and 3650 Ma rim ages with the oldest components of the Meeberrie gneiss is strengthened by the fact that aside from being indistinguishable in age, no other rocks of similar age (i.e. >3600 Ma) exist in Western Australia. If the above interpretation is correct, >4000 Ma crust existed in the vicinity of the oldest Meeberrie gneiss protoliths at ca. 3700 Ma, and there was a close spatial association between both of these components from this time onwards; perhaps also for the Dugel gneiss at ca. 3400 Ma in the case of the younger overgrowth. The early Archean xenocrysts identified by Nelson et al. (2000) suggest that >4000 Ma crust may have continually been involved in regional crustal-forming processes as late as 2650 Ma. This suggests that the known populations of >4000 Ma detrital zircons in Western Australian sediments are locally derived. The close proximity of these potential sources strengthens the hope that rocks older

than 4000 Ma may yet be identified in Western Australia.

6.4. Sources of Jack Hills metasediments and deposition age

Previous studies have identified several detrital zircon populations in the Narryer Terrane, including >4300, 4200, and 4150 Ma (Maas et al., 1992; Wilde et al., 2001) and >3800, 3750–3600, 3500–3300, and 3100–3050 Ma (Nutman et al., 1991). The results of this study have found all of the above populations, as well as two previously unidentified sources from 2750 to 2500 Ma and 2000 to 1600 Ma. Although there must have been multiple sources for the >3800 Ma zircons due to the variable age distribution, no rocks with similar ages have been found in Western Australia, and in fact, no rocks on Earth match the ages >4030 Ma (Bowring and Williams, 1999). Many of the >3800 Ma zircons are euhedral (Fig. 5), however, the extreme rounding of a few grains older than 3800 Ma (e.g. Fig. 5w and x) is indicative of eolian transport (Dott, 2003) that suggests either a distal source for some of this population, or more than one sedimentary cycle.

The 3750–2500 Ma detrital zircons are likely the result of varying contributions from all of the surrounding granitoids, including the Meeberrie, Eurada, and Dugel gneisses, and younger ca. 2650 Ma granitoids.

The 2000–1600 Ma zircons may have originated from rocks of the Paleoproterozoic Capricorn Orogen, an orogenic zone containing Proterozoic sediments, granitoids, and metamorphic rocks located between the Yilgarn and Pilbara cratons (Gee, 1979) (Fig. 1). Previous zircon U–Pb geochronology studies within and near the Gascoyne Complex (Fig. 8a) have identified over forty igneous rocks with Proterozoic ages in the intervals 2008–1945, 1827–1776, and 1674–1619 Ma (Nelson, 1995, 1998, 1999, 2000, 2001, 2002) (Fig. 8b). As the Gascoyne Complex borders the northern margin of the Narryer Terrane (Fig. 8a), and contains rocks of similar age to the three Proterozoic zircons found in Jack Hills sample 01JH63 (Fig. 8b), this is the most likely source for the Proterozoic detritus in the Jack Hills. However, it cannot be ruled out that magmas of these ages may have intruded nearer to or within the Jack Hills and have yet to be recognized.

The presence of 2000–1600 Ma zircons in the Jack Hills sediments is evidence of a previously unknown Proterozoic geologic history of the belt, and requires an explanation that can account for the following three observations: (1) No zircons younger than ca. 3000 Ma have been identified in the West Transect (with the

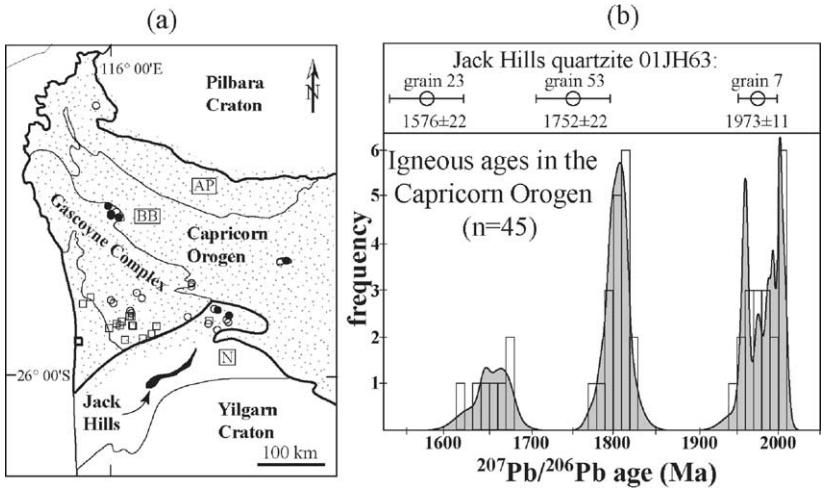

Fig. 8. Proterozoic U–Pb geochronology of the Capricorn Orogen: (a) locations of igneous rocks with assigned ages in the range ca. 2000–1600 Ma based on SHRIMP U–Pb zircon analysis ($n = 45$, references in text). Symbols: (□) 2008–1945 Ma, (◯) 1827–1776 Ma, and (●) 1674–1619 Ma. Abbreviated components of the Capricorn Orogen (stipled): BB: Bangemall Basin, AP: Ashburton Province. N: Narryer Terrane. (b) Histogram and Gaussian summation probability density plot for the 45 ages in (a). Upper symbols are ages of the three Proterozoic zircons identified in sample 01JH63 from this study (errors quoted = 1σ, error bars = 2σ).

exception of 01JH63) during this or prior investigations. (2) West transect sample 01JH63 contains both 1973–1576 and 2736–2590 Ma zircons. (3) East transect samples contain 2724–2504 Ma zircons but no Proterozoic zircons. Assuming that no detrital zircon populations have been missed entirely, three scenarios are possible: (a) Siliciclastic sedimentation in the Archean, as early as ca. 3000 Ma for West Transect sediments (except 01JH63) and as late as ca. 2500 Ma for East Transect samples, followed by a second period of siliclastic deposition in the West Transect after ca. 1600 Ma. (b) Similar to (a), the main deposition of sediments at both transects occurred in the Archean, however, the Proterozoic age sediments were tectonically interleaved in the West Transect after 1600 Ma. (c) All sediments in the Jack Hills were deposited in the Proterozoic, after 1600 Ma. Each scenario above requires the deformation resulting in the vertical attitudes of the beds to have occurred post-1600 Ma, however no tectonic events this young are recognized. The paucity of metamorphic index minerals in the quartz-rich rocks precludes a comparison of metamorphic grade along the transects. Whether there were multiple periods of sedimentation in the Jack Hills, including deposition and/or tectonic transport during the Proterozoic, is difficult to evaluate at present, and will only be resolved by additional mapping and geochronology of the siliciclastic rocks.

7. Conclusions

A record of Early Archean to Proterozoic magmatism is preserved in the form of detrital zircons in the Jack Hills sediments in Western Australia. The CL images and Th–U chemistry of Early Archean zircons described in this study are strong evidence that these zircons are igneous in origin and thus provide dates for magmatic episodes as old as 4400 Ma. Existing data suggest that magmatic events occurred from 4400 to 4250, 4200 to 4000, and intermittently between 4000 and 3800 Ma. These magmatic episodes involved the creation of granitic (sensu latu) zircon-bearing rocks, possibly in environments similar to where these kinds of rocks are being formed in modern settings, but other environments cannot be ruled out. The ability to resolve these early magmatic periods may provide a geologic basis for formal refinements of geochronometric units for subdividing the early Archean time scale.

Xenocrysts and younger overgrowths on >4000 Ma zircons from this and prior studies provide a link between ca. 4000 Ma crust and known rocks in Western Australia. In turn, these rocks demonstrate that Early Archean crust participated in the evolution of the Yilgarn Craton until at least ca. 2650 Ma. Detrital zircons as young as ca. 1600 Ma correlate to known sources, and provide evidence for a previously unrecognized Proterozoic event in the Jack Hills that may place additional constraints on the distribution of >3800 Ma grains within the belt.

The speculations presented in this paper on what Early Archean magmatic environments created the Jack Hills zircons are based on the large amount of literature on the petrogenesis of zircon. In our view, for any proposed scenario to be consistent with all of the features of Early Archean zircons requires the formation of evolved felsic rocks (i.e. granitoid) early in Earth's history, as far back as ca. 4400 Ma.

Acknowledgements

We thank C.R.L. Friend and an anonymous reviewer for critical reviews of the manuscript. We thank Brian Hess (University of Wisconsin) for preparing sample mounts and Matthew Grant (Curtin University) and John Fournelle (University of Wisconsin) for help with the CL imaging. Scott Dhuey's assistance is appreciated during SEM imaging at the University of Wisconsin CN-Tech. We also thank Song Biao and Tao Hua for assistance during analytical sessions on the Beijing SHRIMP. Mary and Matcham Walsh kindly provided hospitality at Mileura Station, W.A. Support for this work was provided by the NSF (EAR-020734), DOE (93ER14389), and the ARC (DP0211706).

Appendix A. Jack Hills sample descriptions

Mineral identification was done in thin section with both a petrographic microscope and by energy-dispersive spectrometry. For most of the accessory minerals listed, it was possible to interpret their origin as either detrital (e.g. Cavosie et al., 2002a) or metamorphic based on morphology and/or texture in

thin section; tourmaline and rutile were two exceptions where the origin of the mineral was ambiguous in many cases; see Fig. 2 for sample locations.

A.1. West Transect samples

Sample W74. A quartz pebble metaconglomerate. Its location is the same outcrop as sample 01JH54 (described in detail below). The W74 zircons in this study are an aliquot from the original separation used by Compston and Pidgeon (1986); additional descriptions of W74 can be found in this reference.

Sample 01JH54. A grey-colored quartz cobble metaconglomerate from the same 2 m-thick layer as W74 (above), that is clast-supported and contains flattened cobbles of quartz up to 19 cm long. The quartz pebbles and cobbles consist of polycrystalline aggregates of interlocking quartz grains that appear to be low-strain, as undulose extinction was rarely observed in the quartz. Accessory minerals include rutile, detrital zircon and chromite, and metamorphic chromian muscovite, actinolite, pyrite, Fe-oxides, and monazite. GPS: Easting = 499,137, Northing = 7,105,849.

Sample 01JH60. A salmon-colored, matrix-supported, quartz pebble metaconglomerate that contains flattened pebbles of quartz up to 1 cm long. The quartz pebbles consist of polycrystalline aggregates of interlocking low-strain grains, similar to 01JH54 (above). Accessory minerals include detrital zircon and chromite, and metamorphic rutile, chromian muscovite, Fe-oxides, monazite, and barite. This sample is the only other conglomerate analyzed from the West Transect, and was collected approximately 25 m southwest of the W74/01JH54 site, in a distinct lithologic unit.

Sample 01JH63. A tan-colored quartzite. The sample consists primarily of granoblastic interlocking low-strain grains of quartz. Accessory minerals include detrital zircon and metamorphic muscovite and barite. This quartzite was collected 58 m south–southeast of the W74/01JH54 site. GPS: Easting = 499,153, Northing = 7,105,794.

Sample 01JH65. A white quartzite. The sample consists primarily of granoblastic interlocking low-strain grains of quartz. Accessory minerals include detrital zircon and metamorphic muscovite. This quartzite was collected 29 m west–southwest from the W74/01JH54 site. GPS: Easting = 499,109, Northing = 7,105,840.

A.2. East Transect samples

Sample 01JH42. A rust-colored quartz pebble metaconglomerate that is matrix-supported and contains flattened pebbles of quartz up to 7 cm long. The quartz pebbles consist of polycrystalline aggregates of interlocking grains, however, unlike the West Transect conglomerates discussed above, the majority of the quartz grains preserve undulose extinction. Accessory minerals include tourmaline, detrital zircon and chromite, and metamorphic chromian muscovite and actinolite. GPS: Easting = 500,036, Northing = 7,106,455.

Sample 01JH43. A friable, rust-colored metasandstone that contains detrital grains of quartz. The quartz grains range from rounded to variably flattened, with many grains exhibiting undulose extinction. Accessory minerals include rutile, detrital zircon and metamorphic muscovite. Located 0.5 m south of 01JH42.

Sample 01JH47. A rust-colored, clast-supported quartz cobble metaconglomerate that contains flattened quartz cobbles up to 10 cm long. The quartz pebbles consist of polycrystalline aggregates of interlocking grains with undulose extinction, similar to 01JH42. Accessory phases include rutile, detrital zircon, and metamorphic muscovite. Located 4.0 m south of 01JH42.

A.3. Additional samples

Sample 01JH32. A white quartzite. Sample consists primarily of interlocking quartz grains with undulose extinction. Accessory minerals include rutile, detrital zircon, and metamorphic andalusite and muscovite. Andalusite grains occur as small aggregates of anhedral grains surrounded by muscovite. GPS: Easting = 499,625, Northing = 7,106,366.

Sample 01JH33. A grey-colored, matrix-supported, quartz pebble metaconglomerate. The quartz pebbles consist of polycrystalline aggregates of interlocking grains with undulose extinction. Accessory minerals include rutile, detrital zircon and chromite, and metamorphic chromian muscovite and andalusite. The andalusite occurs as clusters of anhedral grains surrounded by muscovite. GPS: Easting = 499,692, Northing = 7,106,379.

Sample 01JH36. A white quartzite with mm-scale dark heavy mineral bands defining cross-bedding. The interlocking quartz grains are elongate and exhibit undulose extinction. Detrital chromite occurs throughout

the rock, but is primarily concentrated in the dark bands, along with rutile, detrital zircon, and metamorphic tourmaline, chromian muscovite, and monazite. The 01JH36 is located between the transects, nearer to the East transect. GPS: Easting = 499,947, Northing = 7,106,431.

Sample 01JH100. A white-colored pebble metaconglomerate. The well-rounded quartz pebbles are highly strained, as evidenced by strongly developed undulose extinction in the quartz, whereas the matrix consists of fine-grained granoblastic strain-free quartz. Accessory minerals include tourmaline, detrital zircon, and metamorphic andalusite and monazite. Individual andalusite crystals in this sample are highly elongate, with aspect ratios up to 20:1. GPS: Easting = 531,898, Northing =7,120,057.

Sample 01JH109. Micaceous quartzite. Sample consists primarily of granoblastic grains of strain-free quartz and muscovite. Accessory minerals include rutile, detrital zircon, and metamorphic andalusite. Individual andalusite crystals consist of elongate trains of broken grain fragments that are mantled by muscovite. GPS: Easting = 506,744, Northing = 7,107,613.

Sample 01JH113. A tan-colored quartzite. The sample consists of granoblastic grains of quartz with undulose extinction. Accessory minerals include detrital zircon, and metamorphic muscovite, ilmenite, monazite, and Fe-oxide. GPS: Easting = 507,110, Northing = 7,107,623.

Appendix B. Supplementary data

Supplementary data associated with this article can be found in the online version, at doi:10.1016/j.precamres.2004.09.001.

References

Amelin, Y.V., 1998. Geochronology of the Jack Hills detrital zircons by precise U–Pb isotope dilution analysis of crystal fragments. Chem. Geol. 146, 25–38.

Amelin, Y., Lee, D.-C., Halliday, A.N., Pidgeon, R.T., 1999. Nature of the Earth's earliest crust from hafnium isotopes in single detrital zircons. Nature 399, 252–255.

Baxter, J.L., Wilde, S.A., Pidgeon, R.T., Fletcher, I.R., 1984. The Jack Hills metasedimentary belt: an extension of the Early Archean Terrane in the Yilgarn Block, Western Australia. Australian Geol. Conv., Macquarie University, North Ryde, pp. 56–57 (abstract).

Belousova, E.A., Griffin, W.L., O'Reilly, S.Y., Fisher, N.I., 2002. Igneous zircon: trace element composition as an indicator of source rock type. Contrib. Mineral. Petrol. 143, 602–622.

Bindeman, I.N., Valley, J.W., 2001. Low-δ^{18}O rhyolites from Yellowstone: Magmatic evolution based on analyses of zircons and individual phenocrysts. J. Petrol. 42, 1491–1517.

Black, L.P., Williams, I.S., Compston, W., 1986. Four zircon ages from one rock: the history of a 3930 Ma-old granulite from Mount Sones, Enderby Land, Antarctica. Contrib. Mineral. Petrol. 94, 427–437.

Black, L.P., Kamo, S.L., Allen, C.M., Aleinikoff, J.N., Davis, D.W., Korsch, R.J., Foudoulis, C., 2003. TEMORA 1: a new zircon standard for Phanerozoic U–Pb geochronology. Chem. Geol. 200, 155–170.

Bohor, B.F., Betterton, W.J., Krogh, T.E., 1993. Impact-shocked zircons: discovery of shock-induced textures reflecting increasing degrees of shock metamorphism. Earth Planet. Sci. Lett. 119, 419–424.

Bowring, S.A., Williams, I.S., 1999. Priscoan (4.00–4.03 Ga) orthogneisses from northwestern Canada. Contrib. Mineral. Petrol. 134, 3–16.

Cavosie, A.J., Valley, J.W., Fournelle, J., Wilde, S.A., 2002a. Implications for sources of Jack Hills metasediments: detrital chromite. Geochim. Cosmochim. Acta 66, 125 (abstract).

Cavosie, A.J., Valley, J.W., Dunyi, L., Wilde, S.A., Grant, M., 2002b. 3.7 Ga overgrowths on a 4.33 Ga zircon from Jack Hills: evidence of early crustal recycling. Geol. Soc. Am. Abstr. Prog. 34, 365 (abstract).

Chiarenzelli, J.R., McLelland, J.M., 1993. Granulite facies metamorphism, palaeo-isotherms and disturbance of the U–Pb systematics of zircon in anorogenic plutonic rocks from the Adirondack Highlands. J. Metamorphic Geol. 11, 59–70.

Compston, W., Pidgeon, R.T., 1986. Jack Hills, evidence of more very old detrital zircons in Western Australia. Nature 321, 766–769.

Corfu, F., Hanchar, J.M., Hoskin, P.W.O., Kinny, P., 2003. Atlas of zircon textures. In: Hanchar, J.M., Hoskin, P.W.O. (Eds.), Zircon. Reviews in Mineralogy and Geochemistry, vol. 53, pp. 469–495.

Cox, R.A., 2002. Morphological, chemical, and geochronological techniques for characterizing detrital zircons. In: Lentz, D.R. (Ed.), Geochemistry of Sediments, Sedimentary Rocks: Evolutionary Considerations to Mineral Deposit-Forming, Environments. Geological Association of Canada. Geotext 4, 47–62.

Dott Jr., R.H., 2003. The importance of eolian abrasion in supermature quartz sandstones and the paradox of weathering on vegetation-free landscapes. J. Geol. 111, 387–405.

Dunn, S.J., Nemchin, A.A., Cawood, P.A., Pidgeon, R.T., 2002. Detrital zircons from the Jack Hills metasediments, Western Australia: provenance record of the Earth's oldest material. Geochim. Cosmochim. Acta 66, 201 (abstract).

Elias, M., 1983. Explanatory notes of the Belele geological sheet. Geological Survey of Western Australia, Perth, WA, pp. 1–22.

French, B., 1998. Traces of catastrophe: a handbook of shock-metamorphic effects in terrestrial meteorite impact structures. LPI Contribution No. 954. Lunar and Planetary Institute, Houston, 120 pp.

Froude, D.O., Ireland, T.R., Kinny, P.D., Williams, I.S., Compston, W., Williams, I.R., Myers, J.S., 1983. Ion microprobe identification of 4100–4200 Myr-old terrestrial zircons. Nature 304, 616–618.

Gee, R.D., 1979. Structure and tectonic style of the Western Australian shield. Tectonophysics 58, 327–369.

Gunnarsson, B., Marsh, B.D., Taylor Jr., H.P., 1998. Generation of Icelandic rhyolites: silicic lavas from the Torfajökull central volcano. J. Volc. Geotherm. Res. 83, 1–45.

Hanchar, J.M., Miller, C.F., 1993. Zircon zonation patterns as revealed by cathodoluminescence and backscattered electron images: implications for interpretation of complex crustal histories. Chem. Geol. 110, 1–13.

Hartmann, L.A., Santos, J.O.S., 2004. Predominance of high Th/U, magmatic zircon in Brazilian shield sandstones. Geology 32, 73–76.

Hoskin, P.W.O., 2000. Patterns of chaos: fractal statistics and the oscillatory chemistry of zircon. Geochim. Cosmochim. Acta 64, 1905–1923.

Hoskin, P.W.O., Black, L.P., 2000. Metamorphic zircon formation by solid-state recrystallization of protolith igneous zircon. J. Metamorphic Geol. 18, 423–439.

Hoskin, P.W.O., Ireland, T.R., 2000. Rare earth element chemistry of zircon and its use a provenance indicator. Geology 28, 627–630.

Hoskin, P.W.O., Schaltegger, U., 2003. The composition of zircon and igneous and metamorphic petrogenesis. In: Hanchar, J.M., Hoskin, P.W.O. (Eds.), Zircon. Reviews in Mineralogy and Geochemistry, vol. 53, pp. 27–55.

Kamo, S.L., Reimold, W.U., Krogh, T.E., Colliston, W.P., 1996. A 2.023 Ga age for the Vredefort impact event and a first report of shock metamorphosed zircons in pseudotachylitic breccias and granophyre. Earth Planet. Sci. 144, 369–387.

Kinny, P.D., Williams, I.S., Froude, D.O., Ireland, T.R., Compston, W., 1988. Early Archaean zircon ages from orthogneisses and anorthosites at Mount Narryer, Western Australia. Precambrian Res. 38, 325–341.

Kinny, P.D., Wijbrans, J.R., Froude, D.O., Williams, I.S., Compston, W., 1990. Age constraints on the geological evolution of the Narryer Gneiss Complex, Western Australia. Aust. J. Earth Sci. 37, 51–69.

Kinny, P.D., Nutman, A.P., 1996. Zirconology of the Meeberrie gneiss, Yilgarn Craton, Western Australia: an early Archean migmatite. Precambrian Res. 78, 165–178.

Kober, B., Pidgeon, R.T., Lippolt, H.J., 1989. Single-zircon dating by stepwise Pb-evaporation constrains the Archean history of detrital zircons from the Jack Hills, Western Australia. Earth Planet. Sci. Lett. 91, 286–296.

Liu, D.Y., Nutman, A.P., Compston, W., Wu, J.S., Shen, Q.H., 1992. Remnants of ≥3800 Ma crust in the Chinese part of the Sino-Korean craton. Geology 20, 339–342.

Ludwig, K.R., 2001a. User's Manual for Isoplot/Ex rev. 2.49: A Geochronological Toolkit for Microsoft Excel. Berkeley Geochronological Center Special Publication No. 1a.

Ludwig, K.R., 2001b. SQUID 1.02, A User's Manual. Berkeley Geochronological Center Special Publication No. 2.

Maas, R., McCulloch, M.T., 1991. The provenance of Archean clastic metasediments in the Narryer Gneiss Complex, Western Australia: trace element geochemistry, Nd isotopes, and U–Pb ages for detrital zircons. Geochim. Cosmochim. Acta 55, 1915–1932.

Maas, R., Kinny, P.D., Williams, I.S., Froude, D.O., Compston, W., 1992. The Earth's oldest known crust: a geochronological and geochemical study of 3900–4200 Ma old detrital zircons from Mt. Narryer and Jack Hills, Western Australia. Geochim. Cosmochim. Acta 56, 1281–1300.

Melosh, H.J., 1989. Impact Cratering — A Geologic Process. Oxford University Press, New York, NY, 245 pp.

Meyer, C., Williams, I.S., Compston, W., 1996. Uranium–lead ages for lunar zircons: evidence for a prolonged period of granophyre formation from 4.32 to 3.88 Ga. Meteoritics Planet. Sci. 31, 370–387.

Miller, C.F., McDowell, S.M., Mapes, R.W., 2003. Hot and cold granites? Implications of zircon saturation temperatures and preservation of inheritance. Geology 31, 529–532.

Mojzsis, S.J., Harrison, T.M., Pidgeon, R.T., 2001. Oxygen-isotope evidence from ancient zircons for liquid water at the Earth's surface 4300 Myr ago. Nature 409, 178–181.

Mueller, P.A., Wooden, J.L., Nutman, A.P., 1992. 3.96 Ga zircons from an Archean quartzite, Beartooth Mountains, Montana. Geology 20, 327–330.

Myers, J.S., 1988. Oldest known terrestrial anorthosite at Mount Narryer, Western Australia. Precambrian Res. 38, 309–323.

Myers, J.S., Williams, I.R., 1985. Early Precambrian crustal evolution at Mount Narryer, Western Australia. Precambrian Res. 27, 153–163.

Nelson, D.R., 1995. Compilation of SHRIMP U–Pb zircon geochronology data, 1994. Geological Survey of Western Australia Record No. 1995/3.

Nelson, D.R., 1997. Compilation of SHRIMP U–Pb zircon geochronology data, 1996. Geological Survey of Western Australia Record No. 1997/2.

Nelson, D.R., 1998. Compilation of SHRIMP U–Pb zircon geochronology data, 1997. Geological Survey of Western Australia Record No. 1998/2.

Nelson, D.R., 1999. Compilation of geochronology data, 1998. Geological Survey of Western Australia Record No. 1999/2.

Nelson, D.R., 2000. Compilation of geochronology data, 1999. Geological Survey of Western Australia Record No. 2000/2.

Nelson, D.R., 2001. Compilation of geochronology data, 2000. Geological Survey of Western Australia Record No. 2001/2.

Nelson, D.R., 2002. Hadean Earth crust: microanalytical investigation of 4.4 to 4.0 Ga zircons from Western Australia. Geochim. Cosmochim. Acta 66, A549 (abstract).

Nelson, D.R., Robinson, B.W., Myers, J.S., 2000. Complex geological histories extending for ≥4.0 Ga deciphered from xenocryst zircon microstructures. Earth Planet. Sci. Lett. 181, 89–102.

Nutman, A.P., 2001. On the scarcity of >3900 Ma detrital zircons in ≥3500 Ma metasediments. Precambrian Res. 105, 93–114.

Nutman, A.P., Kinny, P.D., Compston, W., Williams, I.S., 1991. SHRIMP U–Pb zircon geochronology of the Narryer Gneiss Complex, Western Australia. Precambrian Res. 52, 275–300.

Parrish, R.R., Noble, S.R., 2003. Zircon U–Th–Pb geochronology by isotope dilution-thermal ionization mass spectrometry (ID-TIMS). In: Hanchar, J.M., Hoskin, P.W.O. (Eds.), Zircon. Reviews in Mineralogy and Geochemistry, vol. 53, pp. 183–213.

Peck, W.H., Valley, J.W., Wilde, S.A., Graham, C.M., 2001. Oxygen isotope ratios and rare earth elements in 3.3 to 4.4 Ga zircons: ion microprobe evidence for high $\delta^{18}O$ continental crust and oceans in the Early Archean. Geochim. Cosmochim. Acta 65, 4215–4229.

Pidgeon, R.T., 1992. Recrystallization of oscillatory zoned zircon: some geochronological and petrological implications. Contrib. Mineral. Petrol. 110, 463–472.

Pidgeon, R.T., Wilde, S.A., 1998. The interpretation of complex zircon U–Pb systems in Archaean granitoids and gneisses from the Jack Hills, Narryer Gneiss Terrane, Western Australia. Precambrian Res. 91, 309–332.

Pidgeon, R.T., Furfaro, D., Kennedy, A.K., Nemchin, A.A., Van Bronswjk, W., 1994. Calibration of zircon standards for the Curtin SHRIMP II. United States Geol. Surv. Circ. 1107, 251 (abstract).

Plumb, K.A., 1991. New Precambrian time scale. Episodes 14 (2), 139–140.

Rudashevsky, N.S., Burakov, B.E., Lupal, S.D., Thalhammer, O.A.R., Saini-Eidukat, B., 1995. Liberation of accessory minerals from various rock types by electric-pulse disintegration-method and application. Trans. Inst. Mining Metall. 104, C25–C29.

Schidlowski, M., 2001. Carbon isotopes as biogeochemical recorders of life over 3.8 Ga of Earth history: evolution of a concept. Precambrian Res. 106, 117–134.

Tonks, W.B., Melosh, H.J., 1990. The physics of crystal settling and suspension in a turbulent magma ocean. In: Newsom, H.E., Jones, J.H. (Eds.), Origin of the Earth. Oxford University Press, New York, NY, pp. 151–174.

Valley, J.W., 2003. Oxygen isotopes in zircon. In: Hanchar, J.M., Hoskin, P.W.O. (Eds.), Zircon. Reviews in Mineralogy and Geochemistry, vol. 53, pp. 343–385.

Valley, J.W., Chiarenzelli, J.R., McLelland, J.M., 1994. Oxygen isotope geochemistry of zircon. Earth Planet. Sci. Lett. 126, 187–206.

Valley, J.W., Peck, W.H., King, E.M., Wilde, S.A., 2002. A cool early Earth. Geology 30, 351–354.

Vavra, G., Gebauer, D., Schmid, R., Compston, W., 1996. Multiple zircon growth and recrystallization during polyphase Late Carboniferous to Triassic metamorphism in granulites of the Ivrea Zone (Southern Alps): an ion microprobe (SHRIMP) study. Contrib. Mineral. Petrol. 122, 337–358.

Vavra, G., Schmid, R., Gebauer, D., 1999. Internal morphology, habit and U–Th–Pb microanalysis of amphibolite-to-granulite facies zircons: geochronology of the Ivrea Zone (Southern Alps). Contrib. Mineral. Petrol. 134, 380–404.

Watson, E.B., Harrison, T.M., 1983. Zircon saturation revisited: temperature and composition effects in a variety of crustal magma types. Earth Planet. Sci. Lett. 64, 295–304.

Weiblen, P.W., 1994. A novel electric pulse method for obtaining clean mineral separates for geochemical and geophysical research. Eos 75 (Suppl.), 70 (abstract).

Wiedenbeck, M., Compston, W., Myers, J.S., 1988. Single zircon U–Pb ages from the Narryer Gneiss Complex, Western Australia. Geol. Soc. Am. Abstr. Prog. 20, 203 (abstract).

Wilde, S.A., Pidgeon, R.T., 1990. Geology of the Jack Hills Metasedimentary Rocks. In: Ho, S.E., Glover, J.E., Myers, J.S., Muhling, J.R. (Eds.), Proceedings of the Third International Archaean Symposium on Excursion Guidebook. University of Western Australia, Perth, WA, pp. 82–89.

Wilde, S.A., Middleton, M.F., Evans, B.J., 1996. Terrane accretion in the southwestern Yilgarn Craton: evidence from a deep seismic crustal profile. Precambrian Res. 78, 179–196.

Wilde, S.A., Valley, J.W., Peck, W.H., Graham, C.M., 2001. Evidence from detrital zircons for the existence of continental crust and oceans on the Earth 4.4 Gyr ago. Nature 409, 175–178.

Williams, I.S., 1998. U–Th–Pb geochronology by ion microprobe. In: McKibben, M.A., Shanks III, W.C., Ridley, W.I. (Eds.), Applications of Microanalytical Techniques to Understanding Mineralizing Processes. Rev. Econ. Geol. 7, 1–35.

Williams, I.S., Claesson, S., 1987. Isotopic evidence for the Precambrian provenance and Caledonian metamorphism of high grade paragneisses from the Seve Nappes, Scandinavian Caledonides. Contrib. Mineral. Petrol. 97, 205–217.

Wyche, S., Nelson, D.R., Riganti, A., 2004. 4350–3130 Ma detrital zircons in the Southern Cross Granite-Greenstone Terrane, Western Australia: implications for the early evolution of the Yilgarn Craton. Aust. J. Earth Sci. 51, 31–45.